



Title	Significance of the Extracellular Regions in the Rhodopsin of the Fly, <i>Drosophila melanogaster</i>
Author(s)	片野坂, 公明
Citation	大阪大学, 1998, 博士論文
Version Type	VoR
URL	https://doi.org/10.11501/3143774
rights	
Note	

The University of Osaka Institutional Knowledge Archive : OUKA

<https://ir.library.osaka-u.ac.jp/>

The University of Osaka

**Significance of the Extracellular Regions
in the Rhodopsin of the Fly,
*Drosophila melanogaster***

1998

Kimiaki Katanosaka

**Graduate School of Science
Osaka University**

Contents

Contents	-----	p. 2
General Introduction	-----	p. 3
Chapters		
I. N-linked Glycosylation of <i>Drosophila</i> Rhodopsin : Binding Site of the Oligosaccharide Chain and its Functions in the Rhodopsin Maturation	-----	p. 6
Abstract	-----	p. 7
Introduction	-----	p. 8
Materials and Methods	-----	p. 10
Results	-----	p. 14
Discussion	-----	p. 19
Figures	-----	p. 22
II. Analysis of the Light-enhanced Retinal Degeneration Induced by a Mutation in the Second Extracellular Loop of Rhodopsin	-----	p. 30
Abstract	-----	p. 31
Introduction	-----	p. 32
Materials and Methods	-----	p. 34
Results	-----	p. 36
Discussion	-----	p. 42
Figures	-----	p. 46
References	-----	p. 68
Abstract (in Japanese)	-----	p. 76
Acknowledgments	-----	p. 79

General Introduction

Vision is one of the most important senses with which animals get a great deal of information from the external environment. In a visual system, the molecules called visual pigments, which are represented by rhodopsin, absorb light at the first step of phototransduction. Light-activated pigment initiates a sequential molecular event leading to a change in plasma membrane conductance.

In photoreceptor cells, a large amount of visual pigments accumulates in the specialized photoreceptive membranes forming such characteristic structures as closely packed stack of disk-shaped sacs in vertebrate or stack of microvilli in invertebrate. These membrane structures are important for the effective capture of photon and the high sensitivity of photoreceptor cells to light. In addition, these structures are also important for phototransduction, since they contain most proteins employed in the phototransduction.

In the fly, each ommatidium, a unit of compound eye, contains a set of eight photoreceptor cells (R1-8). Each cell projects tightly packed stack of microvilli called "rhabdomere" into the lumen of a circle formed with the photoreceptor cells.

In both *Drosophila* and human, rhodopsin mutations often cause the degeneration of photoreceptor structure (Scavarda et al., 1983; Kurada and O'Tousa, 1995; Colley et al., 1995; Gal et al., 1996). In human, many rhodopsin mutations result in a progressive retinal dystrophy, retinitis pigmentosa (RP) (Dryja et al., 1990; Humphries et al., 1992; Gal et al., 1996). In *Drosophila*, complete absence of rhodopsin in null mutant allele (*ninaE^{o117}*) leads to rhabdomere degeneration (O'Tousa et al., 1989; Kumar and Ready, 1995). This mutant fly shows decrease in rhabdomere size at eclosion and progressive destruction of microvillous structure of rhabdomeres. The rhabdomere defects are allele-dependent and correlate roughly with the severity of the lesion in the rhodopsin gene (Leonard et al., 1992). More severe rhodopsin mutant expresses much less rhodopsin and results in the more pronounced atrophy. These observations suggest that rhodopsin has an essential role in the development and maintenance of the specialized architecture of photoreceptive membranes, although these structures are quite different between *Drosophila* and human. Molecular mechanism of the retinal degeneration caused by mutant rhodopsin remains unclear. However, these reports suggest that construction and maintenance of photoreceptive membranes need continuous synthesis of normal rhodopsin taking proper structure.

Some previous studies proposed that extracellular regions of rhodopsin are important for its proper folding and/or assembly (Doi et al., 1990; Kaushal and Khorana., 1994). As expected from a hydropathy plot analysis, rhodopsin has seven membrane-spanning α -herices, and is divided into three parts, a membrane-spanning domain, an intracellular domain and an extracellular domain. The former two domains have important functions in light absorption

and phototransduction. The membrane-spanning domain is bound to 11-*cis*-retinal and tunes the absorption spectrum of each visual pigment. The intracellular domain physiologically interacts with other proteins, G-protein, rhodopsin kinase and arrestin, on the intracellular surface. The extracellular domain is composed of an amino-terminal tail and three loop regions that connect two membrane-spanning helices. In this domain, there exist several characteristic structures those are well conserved among visual pigments (Applebury and Hargrave, 1986). First, it contains two cysteine residues which connect the first and the second extracellular loops by forming a disulfide-bond. Generally, the disulfide-bond is important for the protein assembly and largely restricts a conformational capacity of the protein. Also in rhodopsin, a disulfide-bond has an important role in protein assembly (Karnic and Khorana, 1990; Ridge et al., 1995). Second, the extracellular domain contains one or several consensus sequences for asparagine-linked glycosylation (N-glycosylation). They are located at the N-terminal tail of all visual pigments, and at second extracellular loop in some cases. However, the role of N-glycosylation is not yet clear. In *Drosophila* rhodopsin, one possible binding site is found in the second extracellular loop. Finally, there is a highly conserved amino acid sequence in the second extracellular loop of many visual pigments (Applebury and Hargrave, 1986). Because any deletions in this region caused low expression of rhodopsin in culture cells and the remarkable loss of regeneration with retinal, it has been assumed that this region is essential to form normal conformation of rhodopsin (Doi et al., 1990).

In this thesis, I present a series of investigations carried out to understand the importance of the N-glycosylation and the second extracellular loop of rhodopsin by the use of *Drosophila melanogaster*. To study the protein synthesis *in vivo*, using mutation analysis, it is very important that proteins are expressed in their native cells rather than in other heterologous expression systems, because the proteins are often processed by the cell specific manner and mature using protein-specific chaperone-like proteins (Baker et al., 1994; Ferreira et al., 1996). We thus use *Drosophila*, in which null mutant of rhodopsin has been isolated, and the transgenic mutant can be constructed easily.

In Chapter I, I determine the accurate site for N-glycosylation in *Drosophila* rhodopsin, and demonstrate that it plays essential role in late stages of rhodopsin maturation. In Chapter II, I describe the detailed analysis of the retinal degeneration that occurs in a mutant carrying a point mutation in the second extracellular loop of rhodopsin. Although, this region does not undergo N-glycosylation, the results demonstrated that the mutation in the second loop leads photoreceptor cells into light-enhanced degeneration.

Chapter I

N-linked Glycosylation of *Drosophila* Rhodopsin : Binding Site of the Oligosaccharide Chain and its Functions in the Rhodopsin Maturation

Abstract

Two mutant rhodopsins, whose putative N-glycosylation sites (Asn20 and Asn196) are alternatively replaced by isoleucine, were synthesized using both a cell-free translation system and transgenic flies (*ninaE^{N20I}* and *ninaE^{N196I}*). In these systems, I examined whether each mutant opsin undergoes N-glycosylation or not. Furthermore, to determine the step of rhodopsin metabolism in which the N-glycosylation is required, I compared the protein level at each step of mature and immature rhodopsin in the transgenic flies. In the cell-free system, N20I opsin was less glycosylated than N196I. Immature N196I opsin expressed in *ninaE^{N196I}* fly was glycosylated like immature wild-type opsin in the normal fly. On the contrary, the immature opsin of N20I was not glycosylated in *ninaE^{N20I}* fly. From these results, I concluded that Asn20 is a unique site for the N-glycosylation of *Drosophila* opsin *in vivo*. In addition, since the maturation of rhodopsin lacking Asn20 was greatly inhibited between the immature intermediate in the rER and mature rhodopsin, the glycosylation plays an important role especially in the protein maturation provably after chromophore binding step in the rER. These results provide the first direct evidence showing that rhodopsin N-glycosylation is involved in the maturation process of rhodopsin.

Introduction

Asparagine-linked (N-linked) glycosylation is often observed in the secretory and membrane proteins, including visual pigments. The extensive studies on the roles of glycosylation have been carried out, and elucidated their roles as the recognition determinants for the cell-protein and cell-cell interaction (reviewed by Lis and Sharon, 1993). In addition to these extracellular functions of oligosaccharide chain, another role of glycosylation played in the intracellular event is recently noted. For instance, correct folding and subcellular distribution require glycosylation in several kinds of proteins (reviewed by Helenius, 1994; Fiedler and Simons, 1995).

Visual pigment, rhodopsin, is a light-sensitive membrane protein. It is composed of an apoprotein moiety, called opsin, and a covalently bound 11-*cis*-retinal. In the vertebrate, rhodopsin undergoes N-glycosylation (Hargrave, 1977). Microscopic analysis of the frog retina revealed that tunicamycin, a drug that blocks the N-glycosylation, inhibits the disk morphogenesis and the incorporation of the newly synthesized opsin into rod photoreceptor outer segment (ROS) (Fliesler et al., 1984; Fliesler et al., 1985; Fliesler and Basinger, 1985). Although these data suggest that N-glycosylation of rhodopsin is required for rhodopsin localization to ROS, other studies using tunicamycin on the bovine rhodopsin contrarily suggest that glycosylation is not essential for its proper localization (Plantner et al., 1980; Kaushal et al., 1994). Thus, the role of rhodopsin N-glycosylation is still confused.

In contrast to vertebrate rhodopsin, fly rhodopsin is not glycosylated in its mature form (De Couet and Tanimura, 1987; Huber et al., 1990). However, it was recently found that, the glycosylated opsin, instead of nonglycosylated mature rhodopsin, is accumulated in the carotenoid-deprived fly (Ozaki et al., 1993; Huber et al., 1993). Because carotenoid is a precursor of rhodopsin chromophore, 3-hydroxyretinal, the glycosylated opsin in the carotenoid-deprived fly is an immature intermediate of rhodopsin before binding chromophore. The intermediate stays in the rough endoplasmic reticulum (rER) presumably due to improper folding of the peptide. By giving chromophore to the deprived fly, the intermediate binds chromophore, takes correct conformation, and is exported from rER. The oligosaccharide chain of the intermediate is then trimmed during the transport from rER toward photoreceptive membrane, and completely removed when it reaches the photoreceptive membrane as a mature rhodopsin. These characteristics of fly rhodopsin suggest that the oligosaccharide chain of rhodopsin is not needed after maturation, but may function in the pathway of its synthesis and transport. Therefore, glycosylation of fly rhodopsin would be one of the best

systems to elucidate the role of glycosylation in protein synthesis and transport.

N-glycosylation generally requires a consensus amino acid sequence, Asn-X-Ser/Thr (where X is any amino acids) (Marshall, 1972). Oligosaccharide chains are covalently linked to the first Asn residue in the sequences. According to the above rule, *Drosophila* rhodopsin contains two putative N-glycosylation sites, Asn20 and Asn196 (O'Tousa et al., 1985; Zuker et al., 1985). In the previous study, O'Tousa constructed the transgenic fly, Δ Asn20 (designated *ninaE^{N20I}* in this thesis), in which Asn20 of rhodopsin is replaced by isoleucine (N20I) to eliminate one of two possible glycosylation sites (O'Tousa, 1992). In the transgenic fly, the amount of mature rhodopsin is remarkably reduced, while opsin mRNA level is equal to that in the wild-type control. A trace amount of N20I rhodopsin, however, appears to function normally to initiate the phototransduction cascade. These results indicate that the substitution of Ile for Asn20 does not cause a defect in the phototransduction, but affects the synthesis or degradation of rhodopsin. However, some problems still remain. First, there is no evidence indicating that Asn20 is actually glycosylated in immature rhodopsin, and whether Asn196 also undergoes glycosylation or not. Furthermore, it is obscure how and in which step of the rhodopsin metabolism the glycosylation functions.

In order to answer the above questions about rhodopsin glycosylation, I took the next four strategies. (1) I utilized the cell-free translation system to get biochemically detectable amount of mutant rhodopsins. Using the system, I examined *in vitro* whether the mutant rhodopsins lacking each putative glycosylation site can bind oligosaccharide chain. (2) I constructed a new transgenic fly, *ninaE^{N196I}*, in which the other putative glycosylation site, Asn196, is replaced by Ile. Using the fly, I examined whether Asn196 undergoes the glycosylation or not. Since N196I rhodopsin still possesses a single glycosylation site at Asn20, the result would also demonstrate whether Asn20 can be glycosylated or not. (3) I attempted to detect the N20I rhodopsin in *ninaE^{N20I}* fly and elucidated whether Asn20 is glycosylated or not *in vivo*. (4) To know the step of the rhodopsin metabolism in which glycosylation is implicated, I examined the expression level of rhodopsin during its maturation in the two transgenic flies, *ninaE^{N20I}* and *ninaE^{N196I}*.

Materials and Methods

Animals

All experiments were carried out on white-eyed (*w*) *Drosophila melanogaster* (Oregon R). In this thesis, I term the white-eyed stock (*w*) without any other mutation "wild-type". Fly stocks were obtained from Dr. K. Isono and Dr. J. E. O'Tousa. Transgenic flies, *ninaE^{N20I}* and *ninaE^{N196I}*, were constructed in J. E. O'Tousa's laboratory. Methods on the construction of *ninaE^{N20I}* were previously described (O'Tousa 1992), and were used for the construction of *ninaE^{N196I}*, too. *ninaE^{N196I}* was first constructed as a red-eyed mutant, carrying normal white (*w⁺*) gene in the genetic background. In the present study, I replaced the X-chromosome carrying *w⁺* gene with the mutant *w* allele to get white-eyed *ninaE^{N196I}*.

Fly stocks were ordinarily maintained at 25 °C on a carotenoid-rich medium (6% yellow corn meal, 5% dry yeast, 3.2% sucrose, and 0.5 - 1.5% agar) under a 12 hr light: 12 hr dark cycle of fluorescent lighting at intensity of 50 lux. Carotenoid deprivation was achieved by raising flies from egg to adult on a medium composed of 10% dry yeast, 10% sucrose, 0.02% cholesterol and 1 - 2% agar.

Unless specified, flies used for experiments were kept in a constant darkness from third instar larva to adults in order to minimize the light-dependent damage of rhodopsin and photoreceptor structure. To rear the flies in a constant darkness, the feeding vials were kept in a can with a lid, and subcultured under dim red light.

Cloning and mutagenesis of opsin cDNA

Poly(A)⁺RNAs were isolated from *Drosophila* heads by the oligo-dT-cellulose column, and reversetranscribed using poly-dT sequences added to the end of linearized pUC9 vectors as a primer. From these single strand cDNAs, the cDNA encoding opsin was amplified using the polymerase chain reaction (PCR) with the vector primer (M13 Primer RV, Takara) and a synthetic oligonucleotide primer against the coding region of the N-terminus of the opsin (according to O'Tousa et al., 1985, Zuker et al., 1985), which is introduced EcoRI restriction site to the 5' terminus. A single fragment was amplified and inserted into pBS vector (Stratagene) using EcoRI and HindIII sites. The sequence of the cDNA clone, which include the whole coding sequences and full-length of the 3' noncoding-region (O'Tousa et al., 1985, Zuker et al., 1985), was confirmed by the dideoxynucleotide chain-termination method (Sanger et al., 1977) using Thermo Sequenase Fluorescent Labeled Primer Cycle Sequencing Kit (Amersham).

cDNAs which encoding the mutant opsins lacking putative N-glycosylation site were constructed using mismatched oligonucleotides as primers for the PCR (5'-

GTGACCTTGTCCACCACCGATCCAA(<-T)TGGAC-3' N20I, : 5'-CGAGGTCAGGA(<- T)TACCCTCCG-3' ; N196I). These primers included the coding sequences for residues 18-28 and 194-199 of opsin, respectively, and contained single replacements from the residues in the parentheses to others (bold letters), which cause substitution of Ile for Asn20 or Asn196. Then the complete cDNA of N20I and N196I were prepared by the replacement of the partial fragments of the wild-type cDNAs with the mutant cDNA fragments digested at suitable restriction sites : EcoRI-Tth111I for N20I, EcoT38-BstEII for N196I. These cDNAs were inserted into the pBS vectors. The sequences of the mutant cDNAs were confirmed by the sequencing as described above.

In vitro translation and glycosylation

cDNAs encoding wild-type or mutant rhodopsins were cloned into the transcription vector pBS downstream of the T7 transcriptional promoter. RNAs were transcribed from the linearized pBS clones and 5'-capped by the mCAP™ mRNA Capping Kit (Stratagene) according to its instruction manual. The presence of 5'cap structure (5' 7meGppp5'G) has been shown to enhance the translation efficiency of eukariotic mRNA by a rabbit reticulocyte lysate. RNAs derived from 0.15 mg of pBS were translated per reaction, in the presence of [³⁵S]methionine (293.0-445.8KBq per reaction, 39.9-44.1TBq/mmol, ICN biomedicals and Du pont) in the rabbit reticulocyte lysate methionine L-[³⁵S] Translation Kit (Du pont) supplemented canine pancreatic microsome (1ml per reaction, Du pont). Translation reactions were carried out at 20 °C for 3.0 hr (for Figure 2A) 3.5 hr (Figure 2B) or 2 hr (Figure 3). Radiolabeling accompanied with the translation were terminated by the addition of cold methionine or placing on ice. Then, the microsome membranes supplemented into the reaction mixtures were precipitated by the centrifugation at 15,000 x g for 30 min at 4°C. The membranes were solubilized in the SDS loading solution (2.3% SDS, 5% 2-mercaptoethanol, 5% glycerol, 62.5mM Tris-HCl [pH6.8]), and incubated at 37°C for 1 hr, followed by SDS-PAGE. For the control experiment, translation was carried out without the microsome membranes or mRNA. In that case without microsome membranes, after the termination of the translation and centrifugation, the supernatant was directly mixed with 4xSDS loading solution and incubated at 37°C for 1 hr, then aliquot was subjected to SDS-PAGE.

Preparation of Drosophila retinas

Drosophila retinas were prepared from young adult flies (~24hr after eclosion). To minimize the light dependent damage to rhodopsin and photoreceptors, flies were reared in a constant darkness from lava to adults. Flies for the Figure 5 were reared in the 12L/12D cycle, and prepared under the light. Other retinal samples

of the dark-reared flies were prepared under the dim red light. The methods of the retinal preparation described by former report (Ozaki et al., 1993). Briefly, Compound eyes were hand dissected and immersed in ice-cold/distilled water (100µl). After 10 min on ice, retinas were suspended by pipeting and remove the corneas. The suspensions were centrifuged, and collected the retinal membrane as pellets. The pellets were solubilized in the SDS loading solution and incubated at 37°C for 1 hr, subjected to SDS-PAGEs.

The method of radiolabeling of opsin in flies was described before (Ozaki et al., 1993). 1.8MBq of [³⁵S]methionine (44.1TBq/mmol) was used to feed 10 flies.

Protein analysis

Protein samples were analyzed by SDS-PAGE (Laemmli, 1970) with 12.5% polyacrylamide slab gels. To get autoradiograms, gels were stained with Coomassie brilliant blue R-250, treated with radioactivity enhancer solution (EN³HANCE, New England Nuclear), dried in vacuum drier and exposed to X-ray film (O-mat AR, Kodak) for 3days. For the autoradiogram shown in Figure 2B, the treatment with the enhancer was omitted, and then the dried gel was subjected to exposure against an Imaging plate (Fuji Photo Film) and visualized by the Image Analyzer BAS2000 (Fuji Photo Film).

For immunoblotting, separated proteins by SDS-PAGE were electrophoretically transferred onto polyvinylidene difluoride (PVDF) membranes (Immobilon-P, Millipore), using SDS-containing buffer (0.02% SDS, 100 mM tris(hydroxymethyl) aminomethane, 192 mM glycine, 15% methanol), according to the method described previously (Ozaki et al., 1993). The membranes were incubated with a monoclonal antibody (MAb) (de Couet and Tanimura, 1987) against C-terminal region of the major *Drosophila* opsin, at room temperature for 30 min. Immunoreactive proteins were detected by an avidin-biotin amplification system (Vecstain ABC kit Elite, Vector Lab.).

To remove N-linked oligosaccharide chain from opsin, *in vitro* translation mixture (containing 0.2µl microsomal membranes) or retinal membrane suspension (containing 12 retinas) was centrifuged to yield membrane fraction. The fraction was solubilized in 2 µl of SDS loading solution, diluted to 23 µl by adding n-octylglucoside (2% at final) and peptide-N-glycosidase F (PNGase F, 2.2 mM at final, Boehringer Mannheim) solutions, and incubated at 37 °C for 17 h. The solution was then mixed with 7 µl of 4 x SDS loading solution for SDS-PAGE.

Northern Analysis

Poly(A)⁺ RNA was directly extracted from 50 heads of the each stock of the flies (0-1 day old) by the guanidine thiocyanate method (Chirgwin et al., 1979), combined with the purification with oligo(dT)-cellulose using a QuickPrep Micro

mRNA Purification Kit (Pharmacia). The extracted poly(A)⁺ RNAs were roughly quantified spectrophotometrically. About 150 ng of poly(A)⁺ RNA from each fraction was then subjected to the northern analysis to determine the relative amount of histone H3.3Q mRNA in each fraction. Based on the results, the amount of poly(A)⁺ RNA charged in each lane was readjusted finely to give equal density of histone signal. Poly(A)⁺ RNA was separated on a 1.4% agarose gel containing 6% formaldehyde, vacuum transferred onto a nylon membrane (Hybond-N, Amersham), and fixed on the membrane by UV irradiation. cDNA probe for opsin is derived from PstI-PstI fragment, and labeled with [α -³²P]dCTP by random priming method. Hybridization was carried out at 53°C for 12 h, and the membrane was washed with 2 x SSC at 25°C, followed by washing with 0.2 x SSC containing 0.1% SDS at 60°C. Hybridization signals were detected with an Imaging plate (Fuji Photo Film) and visualized by the Image Analyzer BAS2000 (Fuji Photo Film).

Results

In vitro Synthesis of Wild-Type Opsin

The major *Drosophila* rhodopsin encoded by *ninaE* gene has two possible N-glycosylation sites within the N-terminal (Asn20) and the second extracellular loop regions (Asn196), (Figure 1; O'Tousa et al., 1985; Zuker et al., 1985). To determine the actual N-glycosylation site of immature rhodopsin, I first carried out the *in vitro* synthesis of opsin using a cell-free translation system. Rhodopsin is a membrane protein which has seven transmembrane domains, and is initially synthesized in rER. Generally, N-linked oligosaccharide chains attach to the extracellular domains of the peptide at the lumenal side of rER. In order to enable the peptide integration into the membrane and the N-glycosylation of the peptide, I added the canine microsome membranes to the translation system of rabbit reticulocyte lysate. Using this system, I first examine the synthesis of wild-type opsin (Figure 2A). Without microsomal membrane, a single kind of polypeptide having apparent molecular weight of 36 k was synthesized in this system (Figure 2A, lane 2). On the other hand, no translated product was detected in the control experiment without opsin mRNA (Figure 2A, lane 1). Because rabbit reticulocyte lysate used here does not contain membrane fraction, the products do not undergo post-translational modifications those require rER or Golgi membranes. Therefore, above results indicated that the 36 k peptide is a core peptide of opsin without N-glycosylation.

I next examined the opsin synthesis in the presence of microsomal membranes. As shown in Figure 2A (lane 3), two kinds of polypeptides having apparent molecular weight of 40 k and 43 k, respectively, were synthesized in addition to the 36 k core peptide. To examine whether 40 k and 43 k opsins are N-glycosylated or not, these products were digested with peptide-N-glycosidase F (PNGase F) which cleaves the linkage between asparagine and every type of N-linked oligosaccharide chain (Figure 2B). By this treatment, two upper bands of opsin (40 k and 43 k) completely disappeared, and 36 k core opsin increased instead (Figure 2B, lane 2). This result then indicates that both 40 k and 43 k opsins are N-glycosylated products of 36 k core opsin. *Drosophila* opsin encoded by *ninaE* gene has two possible sites for N-glycosylation. It is therefore most likely that 40 k and 43 k opsins bind one and two oligosaccharide chains, respectively. This presumption was supported by the following experiments using the mRNAs coding N20I and N196I mutant opsins.

In Figure 2B, mature rhodopsin (lane 1) synthesized *in vivo* is electrophoresed with cell-free translated products. It should be noted that 36 k core opsin is a little larger than mature rhodopsin (35 k). This suggests that, during maturation,

rhodopsin would undergo additional modifications which reduce apparent molecular weight from 36 k to 35 k, but it is still unknown what change happen here.

***In vitro* Synthesis of N20I and N196I Opsins**

Using the same system as above, two mutated opsins, N20I and N196I, were synthesized in the presence of microsomal membranes (Figure 3). Asn20 residue of opsin is replaced by isoleucine in N20I mutant, and Asn196 is replaced in N196I. In both N20I and N196I opsins, 36 k and 40 k peptides were synthesized, but 43 k opsin was not detected (Figure 3, *lanes* 2 and 3). Because each of N20I and N196I opsin has one possible site for N-glycosylation, the result indicates that 40 k opsin binds a single oligosaccharide chain at Asn196 or Asn20, respectively. Furthermore, this result strongly supports the previous presumption that 43 k opsin synthesized *in vitro* from wild-type opsin mRNA would have two oligosaccharide chains both at Asn20 and Asn196.

The apparent molecular weight of immature opsin accumulated in rER of the carotenoid-deprived fly is 40 k (Ozaki et al., 1993), which is corresponds approximately to that of the mono-glycosylated opsin synthesized in the cell-free translation system. Although our cell-free translation system does not originated from *Drosophila*, microsomal membranes used in the system are mostly derived from rER, too. It has been shown that the initial structure of oligosaccharide chain and its processing occurring in rER is common in all eukaryotes examined (Kornfeld and Kornfeld, 1985). Therefore, it is highly probable that 40 k opsins synthesized *in vivo* and in the cell-free system have similar ER-type oligosaccharide chains, which are not so different in size each other. This speculation gives us an idea that 40 k intermediate synthesized *in vivo* does not have two small oligosaccharide chains at Asn20 and Asn196, but has a single oligosaccharide chain like 40 k opsin synthesized *in vitro*. As shown in Figure 3, both N20I and N196I opsins can be N-glycosylated *in vitro*. However, 40 k glycosylated opsin of N20I mutant is much less than that of N196I opsin. This result indicates that Asn196 residue of N20I opsin is less easily glycosylated than Asn20 of N196I opsin. Based on these results, I hypothesized that 40 k intermediate of opsin synthesized *in vivo* would bind a single oligosaccharide chain at Asn20, and next examined the hypothesis by the use of transgenic flies.

Opsin Glycosylation in the Transgenic Flies

In the present study, I newly constructed a transgenic fly, *ninaE^{N196I}*, in addition to *ninaE^{N20I}* which has been developed by O'Tousa (O'Tousa, 1992). Because both mutants were constructed over *ninaE^{oI17}*, the null allele of *ninaE*, these transgenic flies express N20I and N196I opsins, respectively, without any

expression of wild-type opsin at all. In *ninaE^{N20I}* fly, it has been reported that the amount of mature rhodopsin is greatly reduced, while mRNA of N20I opsin is expressed as much as that of wild-type opsin in the wild-type control fly (O'Tousa, 1992; Brown et al., 1994). First, I compared the expression level of rhodopsin transcript of *ninaE^{N196I}* with those of *ninaE^{N20I}* and wild-type, by northern blot analysis (Figure 4). Poly(A)⁺ RNA purified from heads of the each strain was electrophoresed and probed with radio-labeled *ninaE* fragments. The total amount of the RNA loaded in the each lane was normalized with the histone mRNA. Opsin mRNA expressed in *ninaE^{N196I}* fly (lane 3) is approximately 1.5-fold more than that in wild-type (lane 1) and nearly equal to that in *ninaE^{N20I}* (lane 2). The difference at transcription level between wild-type and the mutants might reflect a change of expression efficiency of the genes according to the position in the genome, because the P-elements carrying the mutant rhodopsin genes were inserted at random into the genome. However, since both transgenic flies possess the comparable level of rhodopsin mRNA, the lowered amount of rhodopsin in the mutant is likely to result from disturbances of post-transcriptional step of rhodopsin biogenesis.

I next analyzed the rhodopsin synthesis in these transgenic flies at the protein level. I especially focused on the glycosylation of rhodopsin intermediate and its maturation. In the previous study, it was demonstrated that the intermediate of rhodopsin bearing no chromophore is accumulated, when flies are raised in the absence of carotenoid. If flies were given carotenoid and exposed to the light, the intermediate is supplied with chromophore, and then processed into the 35 k mature rhodopsin (Ozaki et al., 1993). Although the mature rhodopsin is not glycosylated, the intermediate accumulating under the carotenoid-deprived condition is known to be N-glycosylated (Ozaki et al., 1993). So I examined whether the intermediate is glycosylated or not in the two transgenic flies. As shown in Figure 5, 40 k peptide is the intermediate of rhodopsin accumulated in the wild-type flies under the carotenoid-deficient condition (Figure 5A, lane 1; Figure 5B, lane 1). Like wild-type flies, carotenoid-deficient flies of *ninaE^{N196I}* also accumulate 40 k intermediate (Figure 5A, lane 3; Figure 5A, lane 5). By digesting these intermediates with PNGase F, the apparent molecular weight of them were reduced to 36 k (Figure 5B, lanes 2 and 6). This result demonstrates that 40 k intermediate of *ninaE^{N196I}*, as well as that of wild-type, is composed of 36 k core peptide and an N-linked oligosaccharide chain. In contrast to *ninaE^{N196I}*, 40 k intermediate was not detected in the carotenoid-deficient *ninaE^{N20I}* flies, whereas 36 k peptide was found instead (Figure 5A, lane 2; Figure 5B, lane 3). Because the apparent molecular weight of this 36 k peptide was not affected by the treatment with PNGase F (Figure 5B, lane 4), it is clear that the intermediate of *ninaE^{N20I}* is not N-glycosylated.

Above results indicate that not Asn196 but Asn20 is essential to form the glycosylated intermediate of 40 k *in vivo*. In addition, *in vitro* experiments also suggested that 40 k peptide of opsin binds a single oligosaccharide chain, and that Asn20 is much more easily glycosylated than Asn196. Based on these results *in vitro* and *in vivo*, I here concluded that the 40 k intermediate of rhodopsin synthesized in the *Drosophila* photoreceptor cell is a glycoprotein binding a single oligosaccharide chain at Asn20.

Synthesis and Maturation of 40 k Intermediate in the Transgenic Flies

We next investigated in which step of rhodopsin synthesis and maturation the oligosaccharide chain is essentially functioning. As described above, the wild-type (Figure 5A, lane 5) and *ninaE^{N196I}* (Figure 5A, lane 7) flies accumulate the glycosylated immature opsin having apparent molecular weight of 40 k, when they are raised under the carotenoid-deprived condition. On the other hand, *ninaE^{N20I}* fly synthesizes the non-glycosylated immature opsin with the molecular weight of 36 k (Figure 5A, lane 6). By providing these immature molecules with chromophore (i.e. raising flies in a carotenoid-rich medium), they proceed in the maturation pathway and processed into the 35 k mature rhodopsin. Figure 5A indicates that the amounts of immature opsin in *ninaE^{N20I}* (lane 6) and *ninaE^{N196I}* (lane 7) are significantly less than that in the wild-type fly (lanes 3). This result indicates that amino-acid substitution at Asn20, as well as that at Asn196, affects the synthesis or stability of immature opsin. However, this reduction of immature opsin would not arise from the loss of the oligosaccharide chain at Asn20 but possibly from some conformational defect in opsin peptides induced by the amino-acid substitution, because the reduction occurs not only in the non-glycosylated opsin of *ninaE^{N20I}* but also in the glycosylated opsin of *ninaE^{N196I}*.

In contrast to the immature opsin, the synthesis of mature rhodopsin is greatly different between *ninaE^{N20I}* and *ninaE^{N196I}* mutants. As well as wild-type flies (Figure 5, lane 1), both *ninaE^{N20I}* and *ninaE^{N196I}* flies produce the 35 k mature rhodopsin (Figure 5, lanes 2 and 3), when they are raised on carotenoid-rich medium. However, the synthesis of mature rhodopsin is largely reduced in *ninaE^{N20I}* compared with *ninaE^{N196I}*. Because no significant difference in the amount of immature opsin can be found between *ninaE^{N20I}* and *ninaE^{N196I}*, this result demonstrates that the defect in N-glycosylation at Asn20 dramatically inhibits the maturation process from the immature intermediate to the mature form of rhodopsin. Furthermore, it should be noted that, in the *ninaE^{N20I}* mutant, the 36 k immature opsin is detectable even when they are raised under carotenoid-rich condition. Because no immature intermediate (40 k) is found in the wild-type nor *ninaE^{N196I}* fly under the same condition, this result again

indicates that the maturation process is largely blocked by the loss of the oligosaccharide chain at Asn20. In Figure 5A, it is also shown that the amount of mature rhodopsin in *ninaE^{N196I}* fly is reduced to approximately 20% of that in the wild-type fly (*lanes 1 and 3*; note that total proteins in *lane 1* is reduced to 20% of those in other lanes). However, this reduction can possibly be explained by the reduction in the immature intermediate of opsin (*lanes 5 and 7*). In conclusion, the present results demonstrate that N-glycosylation at Asn20 would contribute to the acceleration of rhodopsin maturation rather than the synthesis and stabilization of immature rhodopsin.

Discussion

N-glycosylation functions in the many extracellular events and intracellular localization of the proteins. Recent findings indicate that the oligosaccharides are also required for protein maturation (Ou et al., 1993; Hebert et al., 1995). Immature *Drosophila* rhodopsin has N-linked oligosaccharide, which is, however, completely removed during the process of maturation. Although this suggests that the oligosaccharide of opsin may play an important role in its maturation, only a few studies on the glycosylation of *Drosophila* rhodopsin have been reported (O'Tousa, 1992; Brown et al., 1994). In fact, these studies indicate that mature rhodopsin is not synthesized sufficiently when one candidate site for the N-glycosylation is destroyed, but there have not been any evidence exactly demonstrating the number of oligosaccharide chains which bind to opsin and the actual site of its binding. Furthermore, there is no information at all showing which step of maturation requires the N-linked oligosaccharide chain. Because *Drosophila* rhodopsin transiently glycosylated only in an immature form, it is very difficult to isolate sufficient amount of glycosylated rhodopsin for biochemical analysis. In the present study, I first determined the glycosylation site by constructing the mutant opsins lacking possible sites and expressing them both *in vitro* and *in vivo*. The results demonstrated that Asn20 which exists in the extracellular N-terminal region of opsin is the unique site for N-glycosylation. Carbohydrates were biochemically detected from various kinds of visual pigments (Plantner and Kean, 1976; Nashima et al., 1978; Ju et al. 1994), while there are only a few demonstrations showing their existence at the N-terminal region of the visual pigments (Hargrave, 1977; Duffin et al. 1993). However, possible N-glycosylation site in the N-terminal region is conserved in all visual pigments and most G-protein-coupled receptors whose primary structures were so far elucidated. These facts therefore suggest that N-linked oligosaccharide in the N-terminal region may have a common function in the seven-transmembrane receptors belonging to the rhodopsin family. In the present study, I also demonstrated that Asn196 does not undergo N-glycosylation *in vivo*. Nevertheless, many visual pigments contain a consensus sequence for N-glycosylation within the second extracellular loop (for examples Okano et al., 1992: some vertebrate visual pigments; Smith et al., 1993: horseshoe crab, squid and fly rhodopsins). Because any short deletions in this loop region resulted in the formation of misfolded rhodopsins, it is proposed that the loop contains the important information required for the assembly of rhodopsin molecule (Doi et al., 1990). Therefore, this consensus sequence, together with its flanking region, might be conserved to form a correct structure of rhodopsin, not to work as a target

for N-glycosylation.

When *Drosophila* opsin was translated *in vitro*, Asn196 was glycosylated as well as Asn20. This result suggests that N-glycosylation can potentially occur at both sites in rhodopsin. Therefore, it might be presumable that, in the *Drosophila* photoreceptor cells, co-translational binding of chaperone-like proteins to opsin might block the glycosylation of the second site. NINAA, an eye-specific peptidylproline *cis-trans*-isomerase (PPIase) (Shieh et al., 1989; Schneuwly et al., 1989), is one of possible opsin-binding proteins which is specifically distributed in the photoreceptor cells (Stamnes et al., 1991; Baker et al., 1994). However, it is not likely that NINAA alone contributes to the inhibition of glycosylation, because 43 k rhodopsin bearing two oligosaccharide chains is not detected in the *ninaA* mutant (Ozaki et al., 1993). Alternatively, elongating peptide, which is in the process of translation, may take a specific conformation which prevent the co-translational glycosylation of the second site in the photoreceptor cells.

In the previous studies, it has been shown that the synthesis of mature rhodopsin is depressed in the presence of TM (Stark et al., 1991). In addition, the amount of mature rhodopsin is dramatically reduced in the transgenic fly (*ninaE^{N20I}*) whose opsin contains the amino-acid substitution of N20I (O'Tousa, 1992; Brown et al., 1994). Although these results indicate the important role of N-glycosylation in the rhodopsin metabolism, the critical step requiring the N-linked oligosaccharide chain was not clarified. Here, I elucidated that N-glycosylation at Asn20 predominantly functions in the maturation process of rhodopsin (from 40 k to 35 k) rather than the synthesis or stabilization of immature opsin (40 k). However, it should be noted that immature rhodopsin in *ninaE^{N20I}* mutant is significantly less than that in the wild-type fly, although the mutant contains as much immature rhodopsin as *ninaE^{N196I}*. Therefore, we could not completely exclude the possibility that N-glycosylation at Asn20 may also partly contribute to stabilizing or accelerating the synthesis of immature rhodopsin. Further studies using other amino-acid substitutions might be usable to clarify this point.

The 40 k molecule is the earliest intermediate of opsin so far found, which does not bind chromophore yet, possesses an oligosaccharide chain of high-mannose type, and is accumulated in rER (Colley et al., 1991, Ozaki et al., 1993). The present results thus suggest that the oligosaccharide chain at Asn20 would be working at one or several steps between the export of rhodopsin intermediate from rER and the incorporation of mature rhodopsin into rhabdomeric membrane. A possible way to facilitate rhodopsin maturation is that the oligosaccharide chain enables the interaction between opsin peptides and chaperone-like proteins. Recently, in various kinds of cells were found lectin-like proteins, calnexin (Helenius, 1994) and calreticulin (Peterson et al., 1995), which reside in ER and

interact with some glycoproteins. In *Drosophila* photoreceptor cells, it has also been suggested that NINAA (eye-specific PPIase) interacts with rhodopsin in rER and facilitates its biogenesis (Baker et al., 1995). Furthermore, it was shown that NINAA and rhodopsin also colocalize to secretory vesicles (Colley et al., 1991), suggesting that rhodopsin may require NINAA not only in rER but also in its maturation and transport processes. Therefore, one of these proteins may recognize N-linked oligosaccharide chain of rhodopsin to facilitate its maturation. It would be very important to identify proteins those interact with rhodopsin in the maturation process through the oligosaccharide chain.

In *Drosophila*, all data including ours agree that N-glycosylation is essential for rhodopsin maturation. On the other hand, there is no consistency in the role of N-linked oligosaccharides of rhodopsin in vertebrates. In the TM-treated frog retina, nonglycosylated opsin is not normally incorporated in the ROS membrane (Fliesler and Basinger, 1985; Fliesler et al., 1985). Furthermore, mutant human rhodopsin lacking a N-glycosylation site neither takes proper conformation nor reaches the cell surface, when it was expressed in the cultured 293S cells (Sung et al., 1991). In contrast, TM-treatment did not affect the folding and transport of bovine rhodopsin expressed in the cultured COS-1 cells (Kaushal et al., 1994). In the maturation and transport of rhodopsin, not only N-linked oligosaccharides but also other proteins like chaperones would be required. In fact, as well as in *Drosophila*, it is reported that retina-specific NINAA-like protein facilitates the synthesis of vertebrate rhodopsin (Ferreira et al., 1996). Above conflicting results might possibly be ascribed to the presence or absence of such specific molecules as cooperatively function in the rhodopsin maturation. Therefore, as far as investigations of protein maturation, it would be important to examine using the native cells which originally expresses interested proteins.

In this study, I have answered the remaining questions about the position and the significance of N-glycosylation of the major *Drosophila* rhodopsin. Thus, it provides important insights into the role of protein N-glycosylation *in vivo*.

Chapter I

Figures

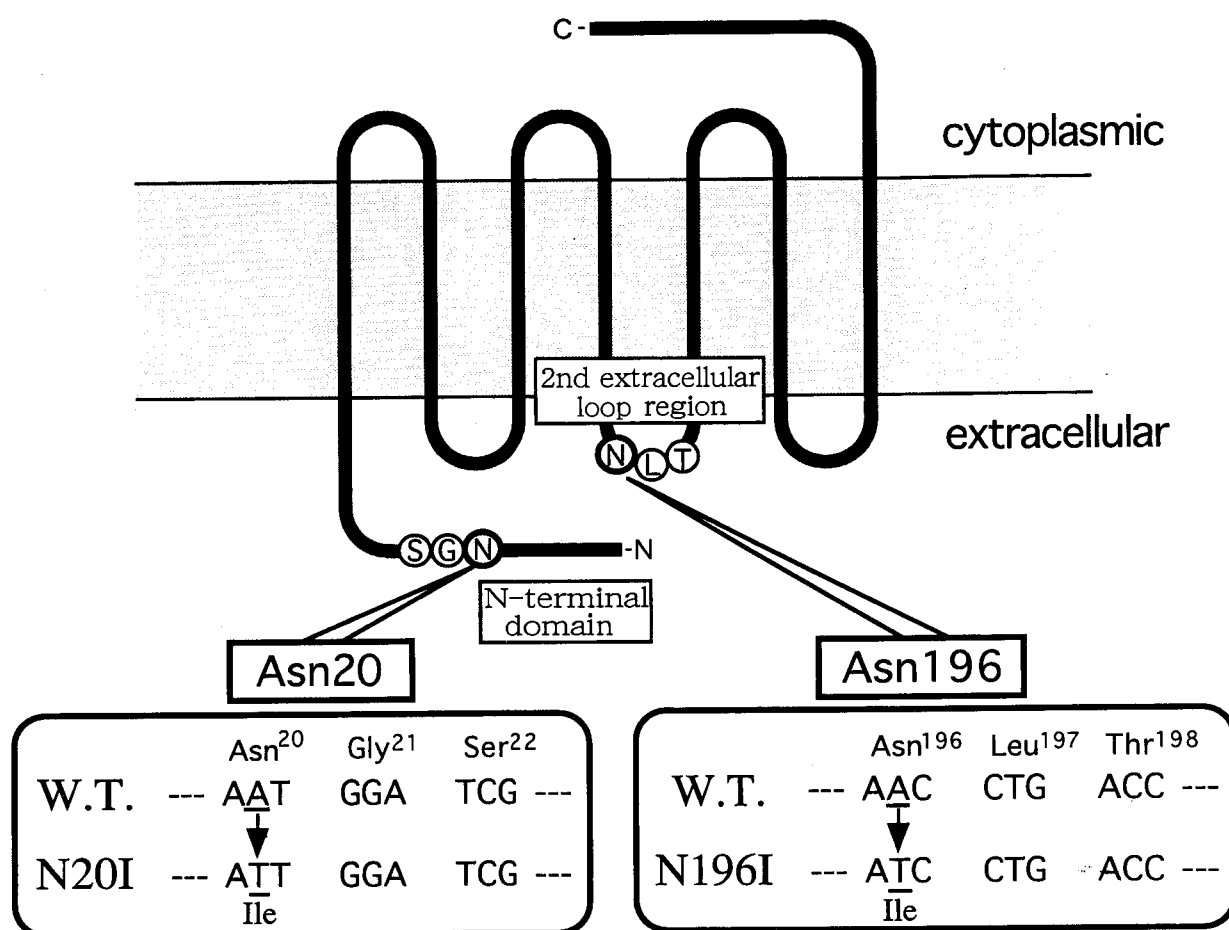


Figure 1. Schematic model of major *Drosophila* rhodopsin.

The figure shows two putative N-glycosylation sites and the mutations used for their substitutions. N-linked oligosaccharide chain can be attached to the Asn residue in the sequences of Asn-X-Ser/Thr (where X is any amino acid). The major *Drosophila* rhodopsin contains two possible glycosylation sites, Asn20 and Asn196, in the N-terminal and the second extracellular loop regions, respectively. *Lower panels* show the partial peptide and DNA sequences of the wild type and two mutant proteins, N20I and N196I. A single nucleotide was changed in each mutant DNA to replace one of these asparagine residues to isoleucine. Details were described in "Materials and Methods".

Figure 2. *In vitro* translation and N-glycosylation of wild-type opsin.

(A) mRNA of wild-type opsin was translated in the reticulocyte lysate translation system supplemented with microsome membranes.

Lane 1, control reaction without mRNA showing that no labeled products are detectable.

Lane 2, another control reaction without microsome membranes. Only a nonglycosylated core peptide (36 k) is detectable.

Lane 3, translation products in the presence of both mRNA and microsome membranes. Two kinds of opsin peptides (40 k and 43 k) is identified in addition to 36 k core peptide.

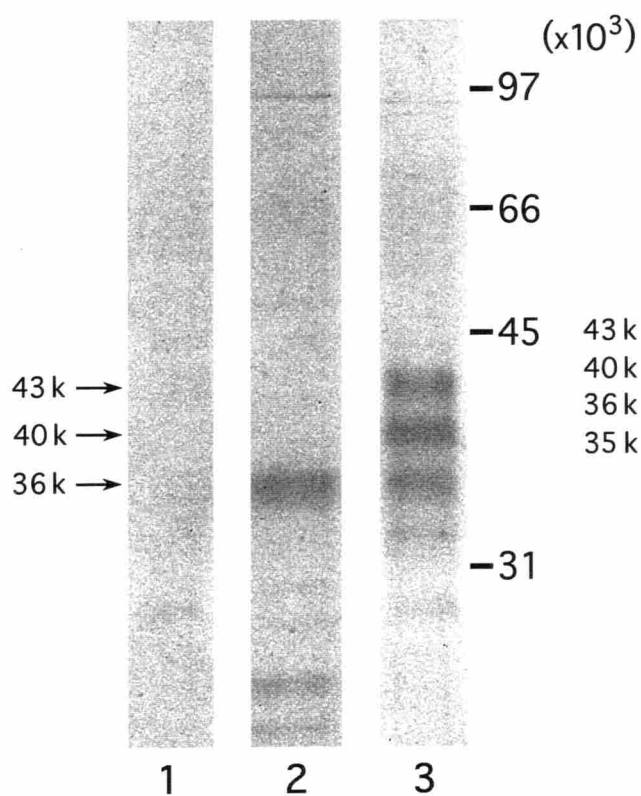
(B) PNGaseF digestion of *in vitro* translation products.

In the absence of PNGaseF, three different bands of opsin peptide are detected at 36 k, 40 k and 43 k (*lane 3*). By digesting with PNGaseF, the apparent molecular weights of two larger opsin peptides (40 k and 43 k) shift to 36 k (*lane 2*). Mature rhodopsin synthesized *in vivo* (35 k) is also electrophoresed in *lane 1*. Note that the core peptide of opsin (36 k) is still larger than mature rhodopsin (35 k).

The positions and molecular weights of protein size markers are indicated on the right.

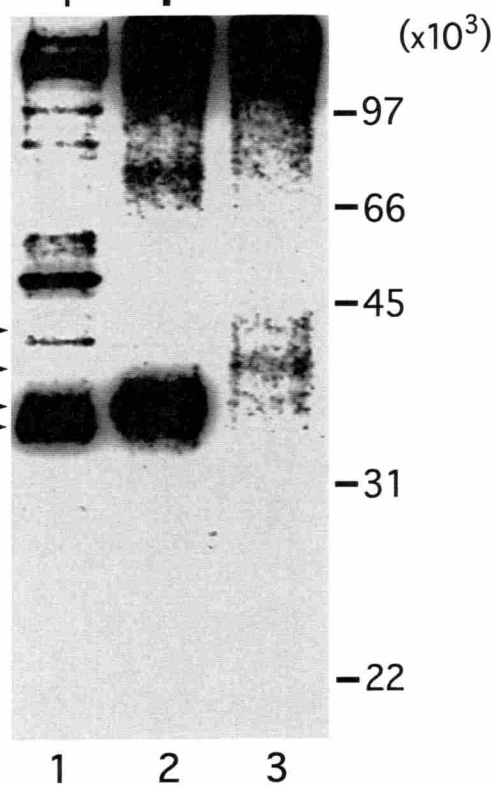
A

mRNA	—	+	+
Memb.	+	—	+



B

<i>in vivo</i>	<i>in vitro</i>
PNGaseF	
+	—



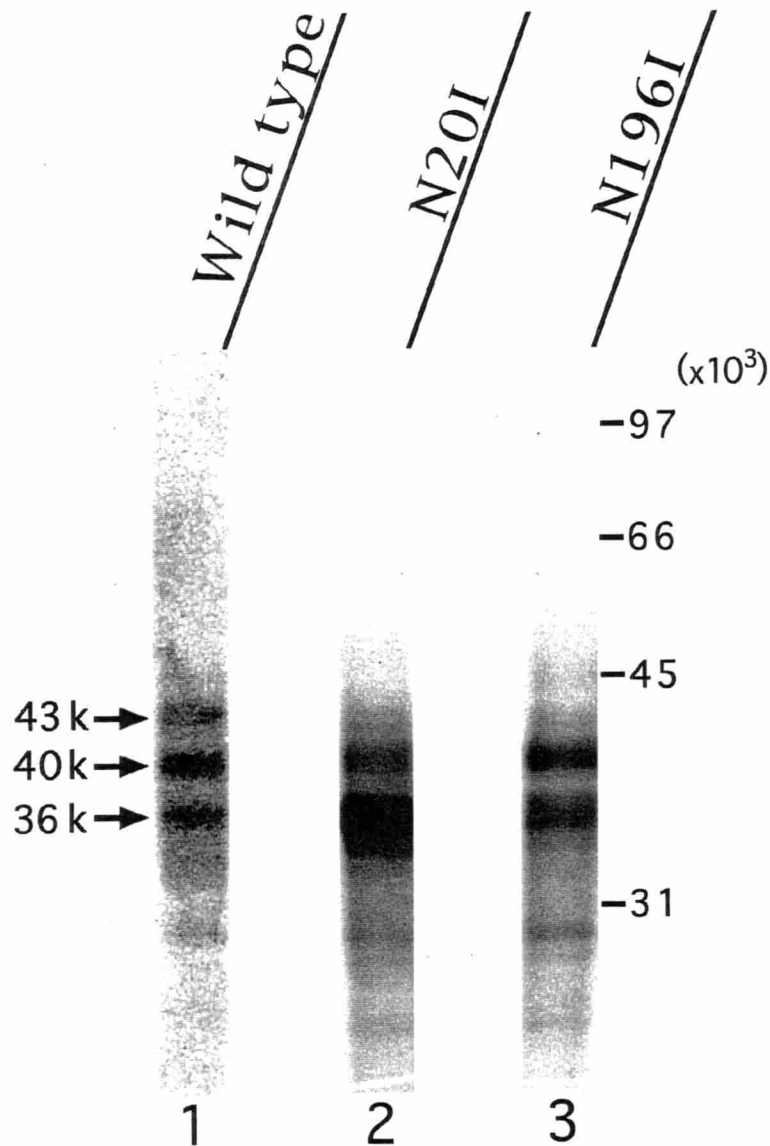


Figure 3. *In vitro* translation and N-glycosylation of mutant opsins, N20I and N196I.

Each mRNA of wild-type (*lane 1*), N20I (*lane 2*) and N196I (*lane 3*) opsins was translated in the reticulocyte lysate translation system supplemented with microsome membranes. The products derived from the mutant mRNAs lack the largest peptide (43 k), while 36 k and 40 k peptides are synthesized from each mutant mRNA. Note that N-glycosylated opsin (40 k) in N196I mutant (*lane 3*) is more abundant than that in N20I (*lane 2*).

The numbers and small bars on the right indicate the positions and molecular weights of protein size markers.

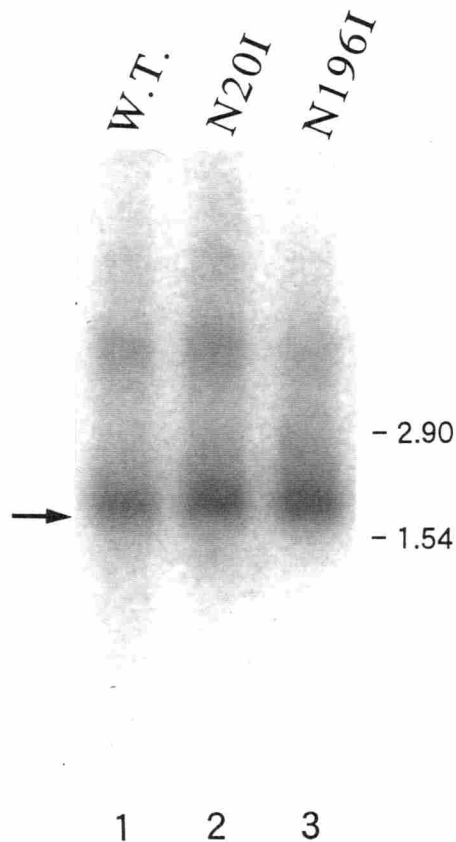


Figure 4. Expression of rhodopsin mRNA in wild-type and the transgenic flies.

mRNA level of major rhodopsin were examined by Northern blot analysis. 150 µg poly(A)⁺RNAs from heads of the each strain were probed with *ninaE* cDNA .

Lane 1, Wild-type

Lane 2, *ninaE*^{N20I}

Lane 3, *ninaE*^{N196I}

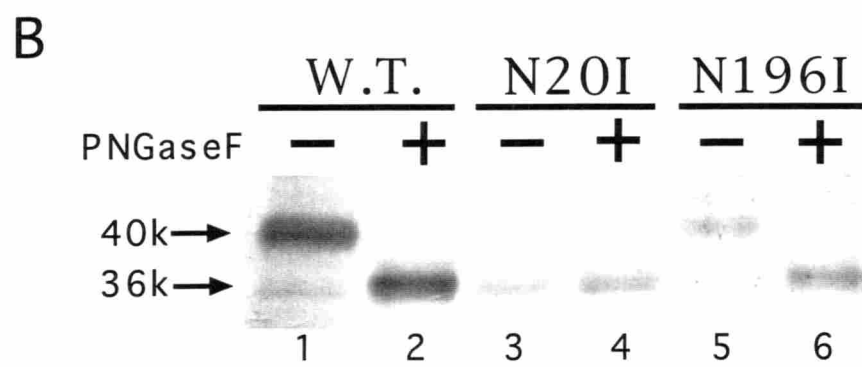
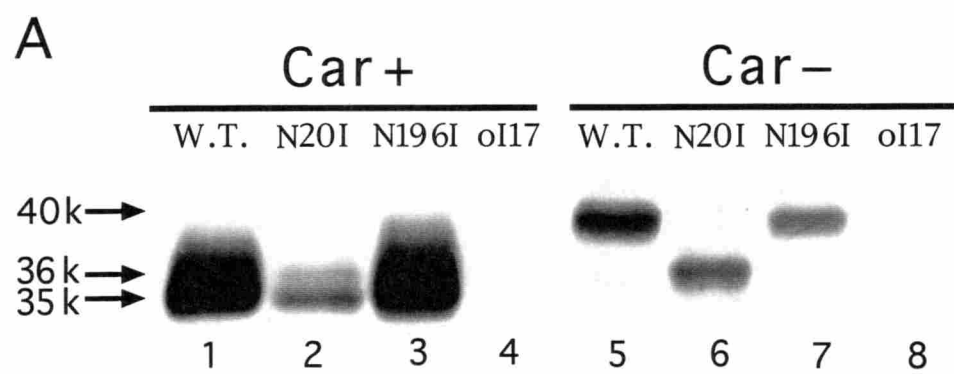
Arrow indicates intact *ninaE* transcripts (1.7 kb).

The numbers on the right side indicate molecular size marker (kb).

Figure 5. Immunoblot analysis of rhodopsin maturation in the *ninaE^{N20I}* and *ninaE^{N196I}* transgenic mutants.

(A) Wild-type (lanes 1, 5), *ninaE^{N20I}* (lanes 2, 6), *ninaE^{N196I}* (lanes 3, 7) and *ninaE^{oI17}* (lanes 4, 8) flies were raised under carotenoid-replete (*Car+*, lanes 1 - 4) or carotenoid-deprived (*Car-*, lanes 5 - 8) condition. In *Car-* condition, 40 k immature opsin is accumulated in the wild-type and *ninaE^{N196I}* flies, whereas 36 k immature opsin is synthesized in the *ninaE^{N20I}* fly. Note that the amount of immature opsin in *ninaE^{N20I}* is similar to that in *ninaE^{N196I}*. In *Car+* condition, the wild-type, *ninaE^{N20I}* and *ninaE^{N196I}* flies yield 35 k mature rhodopsin. In *ninaE^{N20I}*, however, the amount of mature rhodopsin is greatly reduced, and 36 k immature opsin coexists with mature rhodopsin. *ninaE^{oI17}* is a null mutant of major *Drosophila* rhodopsin, showing no opsin peptide in both *Car+* and *Car-* conditions. Extract from 1 eye (lane 1) or 5 eyes (lanes 2 - 8) is loaded in each lane.

(B) N-glycosylation of immature opsin in the wild-type (lanes 1, 2), *ninaE^{N20I}* (lanes 3, 4) and *ninaE^{N196I}* (lanes 5, 6) flies. Retinal extracts from carotenoid-deprived flies were incubated with (lanes 2, 4, 6) or without (lanes 1, 3, 5) PNGaseF. The enzyme reduces the size of 40 k immature opsin to 36 k (wild-type and *ninaE^{N196I}*), but is ineffective against 36 k immature opsin (*ninaE^{N20I}*).



Chapter II

Analysis of the Light-enhanced Retinal Degeneration Induced by a Mutation in the Second Extracellular Loop of Rhodopsin

Abstract

Mutations in rhodopsin gene often cause the retinal degeneration. In this chapter, I report a novel mutation of *Drosophila* opsin that causes light-enhanced retinal degeneration. In Chapter I, I constructed a transgenic fly, *ninaE^{N196I}*, expressing the mutant opsin whose Asn196 in the second extracellular loop is replaced by Ile. When the mutant flies were raised in the constant darkness, they synthesize mature rhodopsin at about 20% of wild-type level just after eclosion. As the flies age, the amount of mature opsin was slowly decreased in the dark. Interestingly, the decrease was greatly accelerated by light. In this process, rhodopsin was subjected to the partial proteolysis. Electron microscopic observation revealed that the mutant shows the age-dependent photoreceptor degeneration, which was also enhanced by light. In the degenerating cells, rhabdomeric microvilli were remarkably disorganized and shortened. Instead, a lot of aberrant membranous structures derived from the microvillar membranes accumulated in the cytoplasm. Finally, the cells were entirely disorganized and probably led to death. The electroretinogram of the mutant, before drastic cell degeneration becomes evident, exhibited normal electrophysiological response to the light, except a defect due to the decrease in rhodopsin. This result excludes the possibility that mutant opsin induces the abnormal activation of transduction system. Probably, mutant rhodopsin and, much more severely, its photoproduct are directly responsible for the photoreceptor cell degeneration.

Introduction

Rhodopsin is a member of the superfamily of the guanine nucleotide binding protein (G-protein) coupled receptors, which contain seven membrane-spanning helices. To understand the structure-function relationships of rhodopsin, many studies using mutant rhodopsins have been carried out both *in vitro* and *in vivo*. One of the reason why those studies are proceeding actively is that many rhodopsin mutations lead to severe dysfunction and degeneration of photoreceptor cells. In human, many rhodopsin mutations result in a progressive retinal dystrophy, retinitis pigmentosa (RP) (Gal et al., 1996). Patients affected by RP initially display night blindness followed by gradual loss of peripheral vision, and loss of all vision, eventually (Gal et al., 1996; Farber and Danciger, 1997). Most of the RPs due to rhodopsin mutations reveal dominant phenotype (autosomal dominant RP, adRP), except a few recessive cases (autosomal recessive RP, arRP) (Rosenfeld et al., 1992, Kumaramanickavel et al., 1994). However, the mechanism by which the mutant rhodopsins cause retinal degeneration is not yet known. To define the pathogenic mechanism of RP, a large number of mutant rhodopsin have been studied *in vitro* and in culture cells, and characterized their molecular defects (Sung et al., 1991; 1993; Min et al., 1993; Kaushal and Khorana, 1994). In these studies, the mutant rhodopsins were characterized in terms of subcellular localization, molecular conformation, binding ability of 11-cis-retinal, absorbance spectrum and G-protein activation efficiency. Thus, it is found that some mutant rhodopsins showed no functional abnormalities *in vitro* or the culture cells (Gal et al., 1996). This would suggest that the authentic mutant phenotype is expressed only *in vivo* and especially requires photoreceptor cell environment. Therefore, in addition to the molecular characterization of the mutant rhodopsins *in vitro*, it is important to investigate the defects resulting from mutations in living animals carrying RP-related mutant rhodopsins.

Drosophila is often used in mutational analysis of protein function *in vivo*, because of its facility of mutagenesis and the construction of the transgenic animals. In *Drosophila*, as well as in human, many rhodopsin mutants have been isolated (Scavarda et al., 1983; Colley et al., 1995; Kurada and O'Tousa, 1995). Most of these mutants are dominant for retinal degeneration (Colley et al., 1995; Kurada and O'Tousa, 1995). In addition, some, but not all, mutations of *Drosophila* rhodopsin correspond to the mutations of human rhodopsin those are implicated in RP. These facts suggest that a similar molecular mechanism works in the process of the retinal degeneration arising from mutations of rhodopsin genes both in human and *Drosophila*.

RP-related mutations reported to date are dispersed over the rhodopsin except

the third extracellular loop (Gal et al., 1996). However, they are somewhat concentrated in the second extracellular loop, and rare in the cytoplasmic loop. In contrast, the most mutant rhodopsins having lesions in the extracellular loops are abnormally accumulated in the rough endoplasmic reticulum (rER) in the culture cell and show low regenerativity with retinal *in vitro* (Doi et al., 1990). Some of them were actually demonstrated to take abnormal conformation by CD spectroscopy (Ridge et al., 1995). From these results, it was proposed that the extracellular domain of rhodopsin would be required for protein folding or assembly rather than direct involvement in the phototransducing activity (Kaushal et al., 1994).

In the study reported in Chapter I, I constructed a new transgenic fly, *ninaE^{N196I}*, so as to eliminate the possible N-glycosylation site in the second extracellular loop. The fly possesses a mutant rhodopsin gene carrying a point mutation that causes a replacement of Asn196 to Ile (N196I). Using the fly, I demonstrated that Asn196 is not concerned with the N-glycosylation. However, the amount of major rhodopsin in *ninaE^{N196I}* was reduced to about 20 % of that in wild-type just after eclosion. It suggests that the loss of Asn196 and/or substitution of Ile affect the rhodopsin metabolism or photoreceptor viability.

In this chapter, in order to explore the effects of the N196I mutation, I investigated the rhodopsin metabolism, photoreceptor cell morphology and electrophysiological photoresponse of the transgenic mutant *ninaE^{N196I}*. Consequently, I demonstrated that the mutation induces a light-enhanced retinal degeneration as a recessive character. Furthermore, I elucidated the time course of morphological changes in degenerating photoreceptor cells, with the detailed electron microscopic analysis.

Materials and Methods

Animals

All experiments were carried out on white-eyed (*w*) *Drosophila melanogaster* (Oregon R). Fly stocks were obtained from Dr. K. Isono and Dr. J. E. O'Tousa. Transgenic flies, *ninaE^{N20I}* and *ninaE^{N196I}*, were constructed in J. E. O'Tousa's laboratory. Methods on the construction of *ninaE^{N20I}* were previously described (O'Tousa 1992), and were used for the construction of *ninaE^{N196I}*, too. *ninaE^{N196I}* was first constructed as a red-eyed mutant, carrying normal white (*w⁺*) gene in the genetic background. In the present study, I replaced the X-chromosome carrying *w⁺* gene with the mutant *w* allele to get white-eyed *ninaE^{N196I}*.

Flies were ordinarily maintained at 25 °C on a carotenoid-rich medium (6% yellow corn meal, 5% dry yeast, 3.2% sucrose, and 0.5 - 1.5% agar).

Lighting conditions

Unless specified, flies used for experiments were kept in the constant darkness from third instar larva to adults in order to minimize the light-dependent damage of rhodopsin and photoreceptor cells in adult compound eyes. To rear the flies in a constant darkness, the feeding vials were kept in a can with a lid, and subcultures were conducted under dim red light. For observation of light-enhanced retinal degeneration, dark-raised young flies (1 day after eclosion) were put into tissue culture dishes, in which moist white filter papers are lying. Then, the dishes were set under the white fluorescent light (500 lux) for indicated period.

Immunoblot analysis

Extracts from retinal membranes were prepared as described in Chapter I. Proteins are separated by SDS-PAGE (Laemmli, 1970) with 12.5% polyacrylamide slab gels. For immunoblotting, separated proteins were electrophoretically transferred onto polyvinylidene difluoride (PVDF) membranes (Immobilon-P, Millipore), using SDS-containing buffer (0.02% SDS, 100 mM tris(hydroxymethyl)aminomethane, 192 mM glycine, 15% methanol), according to the method described previously (Ozaki et al., 1993). The membranes were incubated with a monoclonal antibody (MAb) (de Couet and Tanimura, 1987) or an antiserum (PAb) against C-terminal region of the major *Drosophila* opsin, at room temperature for 30 min. The antiserum was generously presented by Dr. J. E. O'Tousa. Immunoreactive proteins were detected by an avidin-biotin amplification system (Vecstain ABC kit Elite, Vector Lab.).

Conventional Electron Microscopy (EM)

The eyes were prefixed with a fixative containing 2% paraformaldehyde, 2% glutaraldehyde in 0.1M sodium phosphate buffer (pH7.4) for 2 hours on ice. Then the eyes were postfixed with 2% OsO₄ in the same buffer for 2 h on ice. After being dehydrated through the graded ethanol series and embedded in Epon (Quetol 812, Nisshin EM). Ultrathin sections cut with a diamond knife were double-stained with uranyl acetate and lead citrate, and then examined with a JOEL JM1010 electron microscope. The eyes of dark-raised flies were prepared in dim red light until the end of the postfix.

Electron Microscopic Immunocytochemistry

The eyes were fixed with 4% paraformaldehyde, 0.5% glutaraldehyde and 0.05% CaCl₂ in 0.1M sodium cacodylate buffer (CB, pH7.4) for 2 hours on ice, and they were stored overnight in CB at 4 °C. Then the eyes were postfixed with the reduced osmium fixative, containing 1% OsO₄ and potassium ferrocyanide in CB for 30 min on ice (Tamaki and Yamashina 1994). After being dehydrated through a graded ethanol series, the eyes were embedded in LR White resin (London Resin). Ultrathin sections were collected on nickel grids. The sections were first etched overnight with saturated sodium metaperiodate aqueous solution, blocked with 4% bovine serum albumin (BSA) in 0.5M NaCl and 0.25% gelatin in sodium phosphate buffer (PBSG, pH7.4) for 30 min, and then incubated with the antibodies, MAb (1:100 dilution) or PAb (1:25 dilution), in PBSG overnight at 4 °C. Reacted antibodies were detected by incubating with goat anti-mouse IgG conjugated 15 nm-gold (1:25 dilution) (British Biocell) in PBSG for 1 h at room temperature. The sections were stained with uranyl acetate for 3 h at room temperature, and then examined with a JOEL JM1010 electron microscope. The eyes of dark-raised flies were prepared in dim red light until the end of the postfix.

Electroretinogram (ERG)

ERGs were recorded with glass microelectrodes filled with Hoyle's saline. The tip of recording electrode was positioned just beneath the cornea, and the reference electrode was inserted into the brain. Voltage signals were amplified and recorded by means of a high-impedance microelectrode amplifier, a dual-beam oscilloscope, and a thermal array recorder (Nihon Kohden). For light stimuli, 460nm blue- and 530nm green-light from a xenon lamp were used. Flies were dark-raised and quickly immobilized on cover glass with bee's wax under fluorescent room lights.

Results

Age-dependent Changes of Rhodopsin Metabolism in the Mutant

As shown in the Chapter I, the amount of major rhodopsin in the young (within 24h after eclosion) *ninaE^{N196I}* mutant was about 20% of that in wild-type (Chapter 1, Figure 5, lane 3), when flies were kept under the constant darkness. This implies that Asn196 plays some important roles in the rhodopsin metabolism and/or construction of photoreceptor cells. Therefore, I first examined the amount of opsin in the mutant retinæ as a function of ages. Figure 1 displays immunoblot analysis of opsin in the wild-type and mutant flies aged in the constant darkness. After a slight increase in the first day after eclosion, the amount of mature opsin was kept constant for 10 days in both wild-type and *ninaE^{N196I}* flies. However, in the next 10 days, the amount of mature opsin was greatly reduced and became undetectable 20 days after eclosion. Because such remarkable reduction of mature opsin is not observed in wild-type during the period examined, it is characteristic in *ninaE^{N196I}* mutant fly. This mutant phenotype then suggests that the N196I replacement may induce photoreceptor cell degeneration in the dark in an age-dependent manner.

Age-dependent Changes of Photoreceptor Cell Morphology in the Mutant

In order to examine whether reduction of mature opsin is accompanied with a retinal degeneration in the *ninaE^{N196I}* mutant kept in the dark, I investigated the morphology of the mutant photoreceptor cells with a transmission electron microscope (Figure 2-3).

The micrographs in Figure 2 display cross sections through the ommatidia at the level of the R1-6 photoreceptor nuclei. In these sections are observed peripheral photoreceptor cells (R1-6, no marks) and one of central photoreceptor cells (R7, representatively indicated by *asterisk* in Figure 2A). Rhabdomere of the other central photoreceptor cell, R8, is not found in these sections, because they are located at the proximal part of R7 rhabdomere and below the level sectioned here. It has been shown that the peripheral photoreceptors (R1-6) express blue-absorbing rhodopsin encoded by *ninaE* gene, whereas R7 photoreceptor express another rhodopsin absorbing UV light. Just after eclosion, dark-reared *ninaE^{N196I}* has intact photoreceptors (Figure 2B) like those in wild-type (Figure 2A) except the following minor defects. First, the rhabdomere sizes of *ninaE^{N196I}* are distinctly smaller than those of wild-type. The average length of the microvilli in the *ninaE^{N196I}* rhabdomere is roughly estimated at 77% of those of wild-type. Moreover, in the photoreceptor of *ninaE^{N196I}* just after eclosion, the base of rhabdomere occasionally become irregular (Figure 3C), although most have normal regular structures (Figure 3B). In the wild-type fly, neighboring

microvillar membranes are recurving and fused at their loot portion, so that they formed catacomb-like extracellular space (catacomb-like structures, CS) (Kumar and Ready., 1995). In a thin section cut through the proper plane along the axis of the microvilli, CS looks like small membranous loops regularly arrayed along the border between rhabdomere and cytoplasm (Figure 3A and 3D). Another characteristic structure, subrhabdomeric cisternae (SRC), lies adjacently to CS. SRC is a network of a smooth endoplasmic reticulum lying just beneath the rhabdomeres of arthropod photoreceptors (Matsumoto et al., 1989)(Figure 3A and 3D). In the dark-reared *ninaE^{N196I}*, SRC is observed in all rhabdomeres just after eclosion (Figure 3B and 3C). On the other hand, CS is sometimes disordered slightly in the mutant flies (Figure 3C), although, most rhabdomeres show the normal CS (Figure 3B).

10 days after eclosion in the dark, rhabdomere of the wild-type fly is slightly disordered (Fig 2C). Microvillar membranes show small invagination into cytoplasm and the CS become somewhat irregular, while microvilli are packed regularly as those in the fly just after eclosion. In contrast, rhabdomeric structure in the *ninaE^{N196I}* photoreceptors are largely disorganized (Figure 2D). The array of microvilli is largely disordered, and their membranes invaginated into the cytoplasm, making large loops. Catacomb-like structures are completely disrupted, too. However it should be noted that R7 photoreceptor cell of the mutant does not show such abnormal structures as membrane invagination and disruption of CS. Because *ninaE* gene codes for the rhodopsin exclusively expressed in R1-6, but not in R7 and R8, the absence of rhabdomeric disruption in R7 cell in *ninaE^{N196I}* offer a good evidence indicating that severe morphological defects observed in the mutant arise from the N196I replacement in R1-6 rhodopsin. In addition, some photoreceptor cells are characterized by electron-dense cytoplasm and shrinking appearance in the aged flies (10 days after eclosion) of both wild-type and mutant (Figure 2C and 2D, arrows). They are probably degenerated or in unhealthy condition, because similar electron-dense cells are generally observed in the elder (Stark et al. 1988) or the degenerating retina (See below).

These morphological results thus confirm the hypothesis that the reduction of mature opsin in the N196I mutant is accompanied with an age-dependent retinal degeneration.

Light-dependency of the Retinal Degeneration of the Mutant

ninaE^{N196I} mutant shows the phenotype of age-dependent retinal degeneration in the dark. The phenotypes of the retinal degeneration mutants can be categorized into the three types, light-independent, strictly light-dependent and light-enhanced one (Zars and Hyde, 1996). The nature of light-dependency of a retinal

degeneration gives us a good information to estimate the molecular mechanism of the pathology. Therefore, I next examined the light-dependency of the retinal degeneration in the *ninaE^{N196I}* mutant.

To examine the light effect on the retinal degeneration in *ninaE^{N196I}*, I observed the changes in photoreceptor morphology at the several time points under the constant light. The dark-reared young flies (1 day post-eclosion), in which the morphological defects of photoreceptor cells are not evident as yet, were put into constant white-light (500 lux) for the indicated period. As shown in Figure 4 G-I, the rhabdomeres of the wild-type flies are degraded very slowly in the light, and are almost intact even after the irradiation for 48h. In contrast, photoreceptor degeneration in the *ninaE^{N196I}* was remarkably enhanced by light (Figure 4A-F). Light-irradiation for 12 h causes the disorganization of rhabdomeres as severe as that found in the flies kept in the dark for 10 days (Figure 4C). Within 24h after the start of light-irradiation, rhabdomeres are disrupted almost completely. The degeneration is observed not only in the rhabdomeric area but also in the cell bodies of the photoreceptors. In the last stage of degeneration (24-96h, Figure 4D-F), R1-6 cells are vacuolated or shrinking. In these stages, however, the photoreceptor cells reveal heterogeneous features. Some are filled with large and round vacuoles, and others are not (Figure 4D-F). In addition, some are electron-dense, and others are electron-lucent. Electron-dense cells sometimes shrink, while the lucent one often swell out and become loosely packed (Figure 4F). These data probably reflect that cells in this retina are in the different stages of the degeneration process. In all stages, the degeneration occurs only in the R1-6 cells, but not in R7s (Figure 4B-F), as has been observed in the flies kept in the darkness. This therefore indicates that the light-enhanced degeneration is also attributed to the rhodopsin mutation.

Many invaginations of the electron-dense microvillar membranes are observed in the early stage of the degeneration (1-12 h after light-on, Figure 5A-D). In this period, the bases of rhabdomeres are not so smooth as those in wild-type, and membrane structures specific to the subrhabdomeric region (CSs and SRCs) are not evident. The ends of the invaginations are often swollen and electron lucent, and sometimes form membrane loops. Although the long invaginations look membranous narrow tubes in the thin sections, the three-dimensional reconstruction of the similar structures in the rhodopsin null mutant, *ninaE^{o117}*, demonstrated that they are transverse views of doubled membrane sheets (Kumar and Ready, 1995). When a section is cut to obliquely cross the sheets, they reveals faint images (Figure 5A and 5B, *arrow*). In addition, rERs are unusually observed at the subrhabdomeric region of the cytoplasm. They often exists along with microvilli-derived membranes. These membrane invaginations are already evident in the mutant flies exposed to light for 1 h (Figure 5A). The

invaginations then develop and intrude deeply into the cell body (Figure 5B and 5C, 3-6 h exposure to light). Following to the invagination many membranous structures appear in the cytoplasm (Figure 5C and 5D). In these stages, the luminal spaces of the doubled membrane sheets largely grow up, and the membranes probably form extensive network and are folded randomly in the cytoplasm. Therefore, the membranous structures would be observed with various appearances in the thin sections. Such membranes are accumulated more in later stages (Figure 5C and 5D). After 12 hours, the length of microvilli in the remnant rhabdomere are much reduced and the packing become loose. In the later stages (24-96 hours light exposure), massive membrane assemblies including many sacs and lamellae are often observed in the cytoplasm (Figure 6A and C). They sometimes open to the intraommatidial space and release their contents (Figure 4D, E and 6B, D). Presumably these aberrant membranous structures would be derived from the invaginated microvillar membranes. This assumption was assessed by immunocytochemistry. First, I ascertained the localization of the mutant rhodopsin in the healthy-look *ninaE^{N196I}* photoreceptor cells in which the degeneration is not evident as yet. In the young mutant (within 24 h after eclosion), gold particles that represent opsin distribution were densely observed in the rhabdomeres of R1-6 photoreceptor cells (Figure 7A). Few gold particles are found in the cell bodies (Figure 7B). These results indicate that the mutant opsin is correctly targeted to the rhabdomere, and its transport and maturation are not disturbed. Next, I examined opsin distribution in the degenerating photoreceptor of the mutant 24-48 h after light-on. The gold particles were found on some of the aberrant membrane structures (Figure 8), indicating that these membranes are derived from rhabdomeral membranes.

Unusual aspects of degenerating photoreceptors are found in other regions and organelles. The nuclei include many electron-dense particles and lose a fine dot-like staining pattern found in normal nuclei (Figure 9A, B). This implies that the some structural changes are occurring on chromatin. Most of mitochondria are normal at the 12 hours light exposure. However, after 24 hours, as the vacuolation of the cell bodies develop, many mitochondria are swollen and become round shape (Figure 6C and 9B). These changes of the mitochondria seem to be accompanied with the photoreceptor cell degeneration. Furthermore, zonula adhesions (See Figure 4A), by which photoreceptor cells are tightly joined to the neighbors, are lost in the late stage of the degeneration (Figure 4F). Therefore, intercellular adhesions become loose, and secondary pigment cells often invaded through the gap between the photoreceptor cells (Figure 4F). Then, the degenerating cells would be enveloped and phagocytosed by the secondary pigment cells.

Changes of Opsin in the Degenerating Photoreceptor Cells in the Light

I next examined the opsin content in the degenerating mutant photoreceptors after light exposure. In this experiment, two kinds of antibodies were used for immunoblot analysis. Although both are directed against C-terminal tail of rhodopsin, one is a monoclonal ascites (MAb) and the other is a polyclonal antiserum (PAb). When detected with the MAb, mature opsin in the wild-type photoreceptor was kept constant until 48h light, and is gradually reduced during the further irradiation (Figure 10A). In the mutant, however, immunoreactivity of mutant opsin against the MAb is rapidly reduced, and no mature opsin is detectable at 24-36h (Figure 10B). Instead, a faint band having lower apparent molecular weight (MW) becomes visible. These results suggest that mature opsins are gradually subjected to the proteolysis, which yields the opsin with lower MW and lower immunoreactivity against the MAb. Interestingly, the lower band still keeps high immunoreactivity with the PAb at 24h. As shown in Figure 10C, a substantial amount of opsin with lower size is detectable with PAb in the flies exposed to light for 24h, whereas little opsin can be detectable with the MAb. This lower size opsin is stable and still remains at the similar level after 96h, although photoreceptor degeneration is remarkable and rhabdomeres have almost gone in the flies. These results then suggest that the MAb recognized an extremely restricted site in the C-terminal tail of opsin, probably in the most C-terminal end. By the partial digestion of the C-terminal end of opsin, accompanied with rhabdomere disorganization, the epitope for the MAb might be eliminated.

I determined opsin localization in the degenerating *nina^{EN196I}* retinae by immunocytochemistry using both MAb and PAb. Figure 11 displays electromicrographs in which localization of opsin was indicated by gold particles. Because the partially degraded opsin is highly reactive to the PAb but little to MAb, the regions reactive only to the PAb would contain the degraded opsin. On the other hand, the regions reactive with both MAb and PAb contain mature opsin. In the photoreceptors of the *nina^{EN196I}* exposed to light for 48h, gold particles for PAb-reactive opsin are found on the all rhabdomeres examined (Figure 11B). On the other hand, MAb-reactivities are observed in some rhabdomeres but not in others even in a single ommatidium (Figure 11A). These results indicate that partially degraded opsin still stays in rhabdomeres, and again suggest the heterogeneity of the cells in the degree of degeneration.

Electrophysiological Phenotype of *nina^{EN196I}*

Electroretinogram (ERG) was measured to examine the physiological defects of the mutant. ERG is extracellularly recorded mass responses of the eye to the light stimuli. In Figure 12, I compared the ERG of *nina^{EN196I}* with that of wild-type. ERGs were recorded from the young flies reared in the constant darkness. The

ERG amplitude in the mutant is comparable to that of wild-type. Moreover the wave form of ERG was similar to each other except for the absence of the prolonged depolarizing afterpotential (PDA) in the mutant after blue-light stimuli. PDA is derived from the overproduction of photoactivated rhodopsin (metarhodopsin) with blue-light. Reduction of rhodopsin content therefore eliminates the PDA. Absence of PDA in *ninaE^{N196I}* is thus explained solely by the reduced rhodopsin content in the mutant. Moreover, on- and off-transient responses are normally present in the mutant ERG. The on- and off-transients arise from the second order neurons in response to the R1-6 activity. The normal transients in *ninaE^{N196I}* suggest that R1-6 photoreceptor cells make normal synapse to the post-synaptic neurons. As a result, in spite of low level of functional rhodopsin, R1-6 cells are physiologically active and show normal photoresponse.

Phenotype in the *ninaE^{N196I}* Heterozygote

To examine whether the mutant phenotype of *ninaE^{N196I}* is recessive or dominant against wild-type, I check the opsin content in heterozygotes, *ninaE^{N196I}*/wild-type (*N196I* /+) by the immunoblot analysis. In Figure 13, the amount of mature opsin in several kinds of heterozygotes for the rhodopsin gene (*ninaE*) were compared. The heterozygote, *ninaE^{oI17}* /+, has a one copy of *ninaE* gene, because *ninaE^{oI17}* is a null allele due to a partial deletion within *ninaE* gene. The opsin content in this heterozygote (*lane 2*; -/+) has a slightly reduced level of wild-type opsin (*lane 1*; +/+). However, a heterozygote of a wild-type and dominant mutant (*ninaE^{D2}*) alleles shows a great reduction of opsin (*lane 3*; *D2*/+). This reduction is due to interference in the maturation of the wild-type rhodopsin by the mutant protein (Kurada and O'Tousa, 1995). On the other hand, the amount of opsin in the *ninaE^{N196I}* / + (*lane 3*; *N196I*/+) is comparable to that in *ninaE^{oI17}* /+, indicating that *ninaE^{N196I}* mutant gene does not affect the synthesis of wild-type opsin like dominant *ninaE* gene. Therefore, the phenotype of the *ninaE^{N196I}* is recessive for wild-type. In Figure 13, it was also indicated that *ninaE^{N20I}* does not affect the synthesis of wild-type opsin, either (*lane 5*; *N20I*/+).

Discussion

In this chapter, several defects of *ninaE^{N196I}* mutant flies have been revealed. One of the defects of *ninaE^{N196I}* mutant is a low yield of opsin. This mutant possesses mature opsin at 20 % of wild-type level. Many rhodopsin mutants those show the similar phenotype have been reported, and most of those are more severe than *ninaE^{N196I}* (0 - 1.5% of wild-type; Johnson and Pak, 1986). In *ninaE^{N196I}*, the amount of opsin mRNA is comparable to that of wild-type, suggesting that the reduction of opsin level arise neither from the abnormal transcription nor low stability of mutant opsin mRNA. Therefore, the reduced amount of opsin in *ninaE^{N196I}* would result from the aberration at the later stage than translation. A possible interpretation is that intracellular transport of opsin from rER to rhabdomeric microvilli might be disturbed in the mutant. However, the present immunohistochemical studies demonstrated that mutant rhodopsin is normally transported to rhabdomeres and accumulated neither in the cell bodies nor somatic plasma membranes. In addition, abnormal accumulation of cell organelles involved in the protein synthesis and transport was not observed in *ninaE^{N196I}* mutant, although aberrant structures of rER or Golgi body have been reported in *ninaA*, *ninaD* and *DRab1(N124I)* mutants, all of which affect maturation or intracellular transport of rhodopsin (Colley et al., 1991; Satoh et al., 1997). These results, therefore, indicate that N196I rhodopsin is not detained anywhere through the maturation and transport processes. On the other hand, I demonstrated that the amount of 40k immature opsin is reduced in the *ninaE^{N196I}* mutant, compared with that in the wild-type fly. This finding suggests that the immature N196I opsin is less stable than that of wild-type opsin. I therefore assume that N196I mutation would moderately affect the folding process of opsin in rER and the stability of immature opsin on the way of maturation. Possibly, some fraction of N196I opsins might take abnormal conformation, which is readily degraded during the maturation, while the rest are normally processed and transported with the correct conformation.

As discussed above, it is likely that substitution of Ile for Asn196 makes opsin less stable, probably through the incorrect folding of peptide. The primary structure of the moiety flanking Asn196 in the second extracellular loop is well conserved throughout the visual pigments, although Asn196 itself is not found in all visual pigments (Applebury and Hargrave, 1986). The region includes a cysteine residue forming disulfide bond with another cysteine in the first extracellular loop (Karnik et al., 1990). Moreover, several sites for the mutations which cause adRP have been reported in this region (Keen et al., 1991; Gal et al., 1996). Therefore, not the Asn196 alone but the tertiary structure of this moiety

would be responsible for the stability of rhodopsin, as well as for the photoreceptor degeneration discussed below.

Another defect of *ninaE^{N196I}* mutant is the pathology of light-enhanced retinal degeneration. Photoreceptor cells of the mutant gradually degenerated in the age-dependent manner under the constant darkness. Furthermore, the cell degeneration is dramatically accelerated under the constant white-light. Just after eclosion, however, photoreceptor cells in the mutants are almost intact except a little decrease in the size of rhabdomere. In the mutant, the cross-sectional area of a single R1-6 rhabdomere is, on average, reduced to approximately 50-60% of wild-type rhabdomere. It has been reported that other rhodopsin mutants, *ninaE^{P318}*, *ninaE^{P332}* and *ninaE^{P334}*, whose rhodopsin levels are at 0.0004-1.5% of the wild-type, also have small (60-65% of the wild-type) but well-organized rhabdomere. Moreover, in the wild-type fly, carotenoid-deprivation decreases the amount of mature rhodopsin, which is then accompanied with the loss of rhabdomeric size (about 50% of the normal rhabdomere) (Sapp et al., 1991a). These results thus suggest that the change in the rhabdomere size in the *ninaE^{N196I}* mutant would result from the reduction of the amount of resident rhodopsin, which is estimated at about 20% of the wild-type level. In addition, intact rhabdomere of the young mutant fly indicates that the N196I replacement does not largely affect a photoreceptor development, but maintenance of photoreceptor cell structures.

The largest enigma in the retinal degeneration in *ninaE^{N196I}* is why the mutation in rhodopsin leads to the atrophy of photoreceptor cells. As discussed above, simple reduction of the rhodopsin content does not cause the degeneration. A possible answer is that the mutant N196I rhodopsin induces the prolonged activation of phototransduction cascade, which then causes a pathogenic overstimulation of photoreceptor cells. In order to test this hypothesis, I recorded ERGs from the mutant, and compared them with those from the wild-type. The results, however, indicated that the mutant ERG against green-light stimulus is indistinguishable from that of the wild-type. Any difference in the rate of deactivation after light-off is not observed between the mutant and the wild-type flies. This result thus excludes the possibility that the mutant opsin may induce the abnormal activation of phototransduction system, which results in the photoreceptor cell degeneration. In human, three mutant rhodopsins those constitutively activate transducin (a protein in the phototransduction cascade) *in vitro* has been reported (Robinson et al., 1992 ; Gal et al., 1996). One of them is, however, inactivated by phosphorylation and binding of arrestin in the transgenic mice (Li et al., 1995). Furthermore, two other mutants do not cause RP, although they induce light adaptation in the dark probably due to their constant activities *in vivo* (Dryja et al., 1993; Rao et al., 1994). Therefore, these results also suggest

that rhodopsin mutations causing continuous activation of phototransduction system do not induce retinal degeneration.

Recently, it was demonstrated that *rdgC* mutant having defect in the rhodopsin phosphatase shows light-dependent retinal degeneration, even when its phototransduction cascade is blocked by a defect on a protein (DGq or phospholipase C) involved in the cascade system (Steel and O'Tousa, 1990; Vinós et al., 1997). Furthermore, elimination of the C-terminal phosphorylation sites of rhodopsin prevents the photoreceptor cells from degeneration in the *rdgC* mutant, leaving normal activity of phototransduction. These results thus indicate that hyperphosphorylated rhodopsin is a cause of the light-dependent retinal degeneration in the *rdgC* mutant, and may be involved in the retinal degeneration in the *ninaE^{N196I}*, too.

In order to obtain insights into pathology of retinal degeneration, detailed morphological observations of degenerating cells, as well as their biochemical and genetic analyses, would be essential. In this study, I revealed several characteristic changes occurring in the degenerating photoreceptor cells. First, a lot of aberrant membranous structures emerge in the cell body. These structures are likely to be derived from the invagination of the rhabdomeric membranes rather than ERs or Golgi bodies, because they show high immunoreactivity against anti-opsin antibodies and are accompanied with the degradation of microvillar membranes. Second, as the disassembly of rhabdomere advances, opsin is subjected to the limited proteolysis. In the normal cells, microvillar membranes containing rhodopsin are recovered as coated vesicles, and transported to multivesicular and multilamellar bodies located in the cell bodies. Rhodopsin is then degraded in these lysosomal structures (Sapp et al., 1991b). In contrast, immunohistochemical observation indicated that the proteolysis occurs not only in the cell bodies but also in the degenerating rhabdomeres. This result suggests that the degenerating cell may be involved in autolysis, and lysosomes might be collapsed and release their contents including proteases. Thirdly, in the late stage of degeneration, nuclei in bizarre appearance showing structural changes of chromatin are found in some cells. These cells often shrink as found in the apoptotic cells. Apoptosis is in fact reported in the transgenic mice expressing RP-related mutant rhodopsin (Cailliau et al., 1993; Chang et al., 1993). On the other hand, other cells in this stage are vacuolated and have swollen cell bodies and mitochondria. These features are characteristic to the necrosis. Therefore, the retina in this stage looks a mixture of apoptosis-like and necrosis-like cells both proceeding to cell death. Finally, it should be noted that phenotypes of *ninaE^{N196I}* are recessive. This means that a large excess of the mutant rhodopsin would be required to show the mutant phenotypes of the *ninaE^{N196I}*.

Based on above discussion, I here propose a preliminary model for the retinal

degeneration in the *nina*^{EN196I}. In the model, rhodopsin phosphorylation is a key component of the retinal degeneration. Phosphorylation of rhodopsin might accelerate the turnover of photoreceptor membranes. In the homozygous mutants, excess of phosphorylated rhodopsin causes an abnormal acceleration of the turnover, and then disturbs normal protein transport and/or metabolism of the cells. Finally, the cells are wounded and led to death through the necrotic or apoptotic process. To confirm these possibilities, it would be necessary to examine the levels of rhodopsin phosphorylation and membrane turnover in the rhodopsin mutants.

Chapter II

Figures

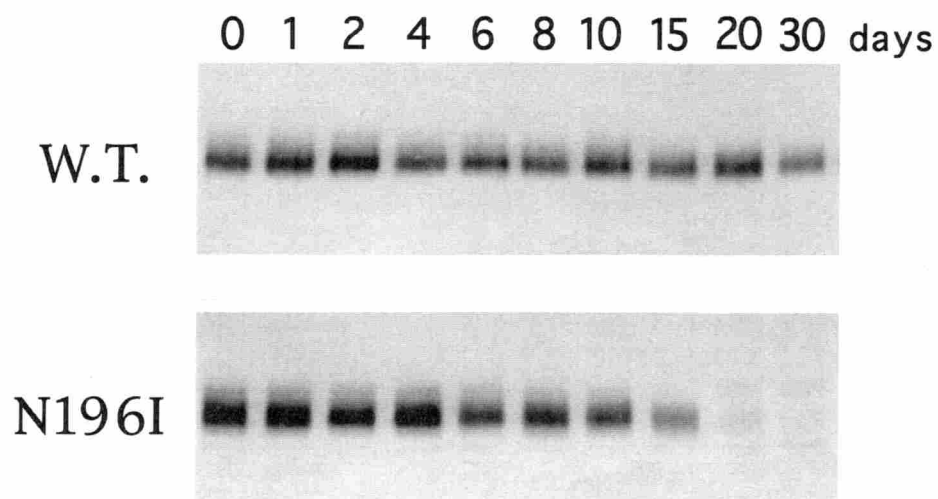


Figure 1. Age-dependent changes of the mature opsin in the constant darkness.

Immunoblot analysis of major opsin in the dark-reared wild-type and *ninaE*^{N196I} flies in different ages. Numbers on the top of the blots indicate ages (days after eclosion). Retinal membrane proteins of the flies were electrophoretically separated and transblotted on the PVDF membranes. The membranes are then incubated with monoclonal anti-rhodopsin antibody (MAb).

Each lane contains the extract from 0.2 eyes in wild-type or 1 eye in *ninaE*^{N196I}.

Figure 2. Age-dependent morphological changes of the photoreceptor cells in the constant darkness.

Electron micrographs of the transverse sections of ommatidia in the dark-reared wild-type and *ninaE*^{N196I} flies.

A, The wild-type ommatidium just after eclosion.

B, The *ninaE*^{N196I} ommatidium just after eclosion.

C, The wild-type ommatidium at 10 days after eclosion.

D, The *ninaE*^{N196I} ommatidium at 10 days after eclosion. Rhabdomeres are remarkably disorganized.

The position of the R7 photoreceptor cell is indicated by *asterisk* in **A** representatively.

Arrows, electron-dense and shrinking cells; *Arrowheads* in **A**, Zonula adhesions;

Scale Bar : 1 μ m

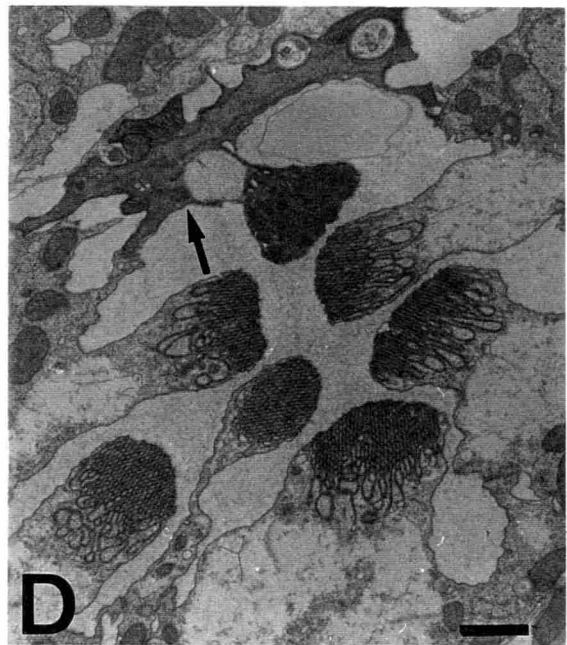
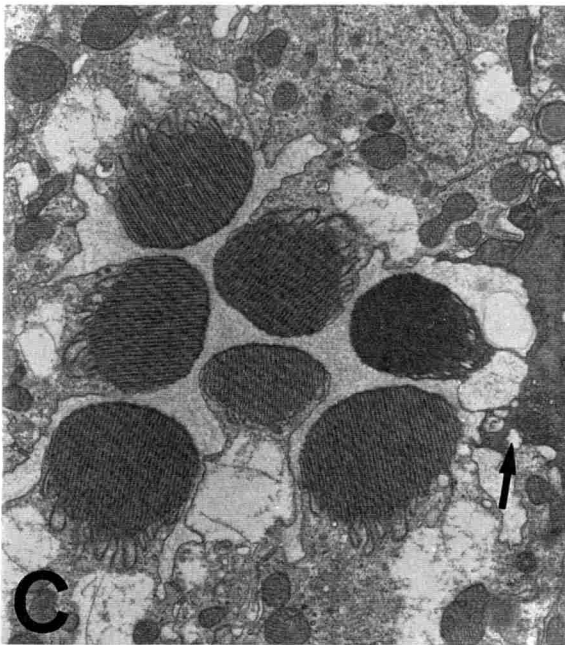
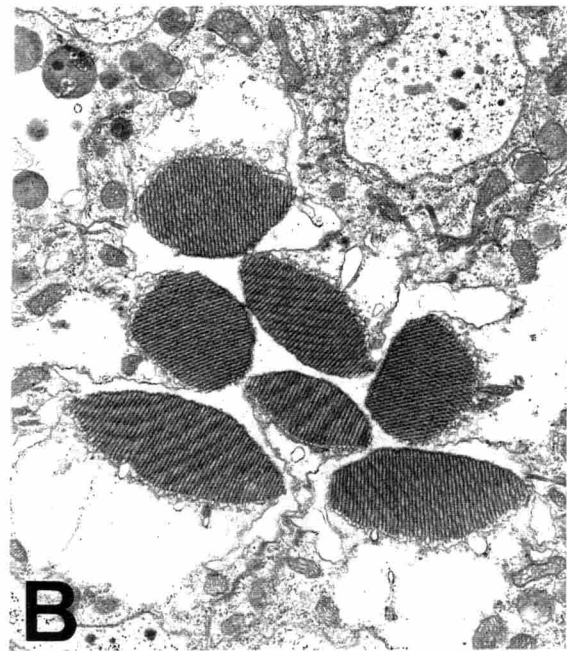
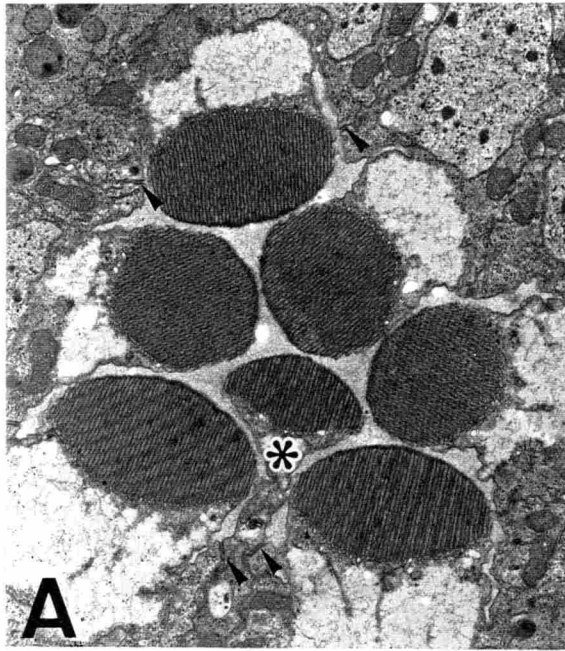


Figure 3. High magnification view of the subrhabdomeric regions.

Electron micrographs of the basal regions of rhabdomeres in the dark-reared wild-type and *ninaE* *N196I* flies just after eclosion.

A, Wild-type

B and **C**, *ninaE* *N196I*

D, Schematic representation of the normal subrhabdomeric regions.

CS, catacomb-like structure; SRC, Subrhabdomeric cisternae

Most photoreceptor cells in *ninaE* *N196I* show normal subrhabdomeric structures as shown in **B**, but some show irregular CS (*arrowheads*) (**C**). SRCs (*arrows*) are observed in **B** and **C**.

M, mitochondria; *Scale Bar*: 250 nm

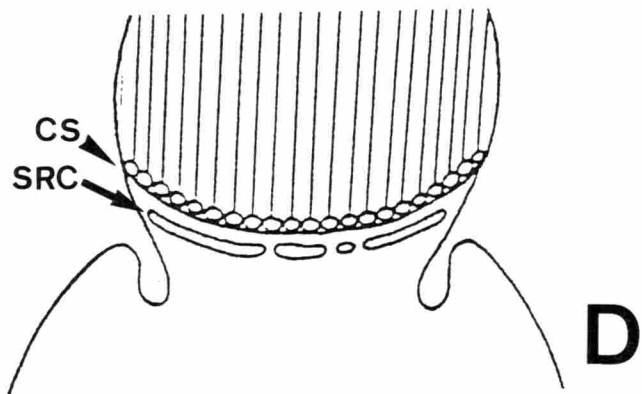
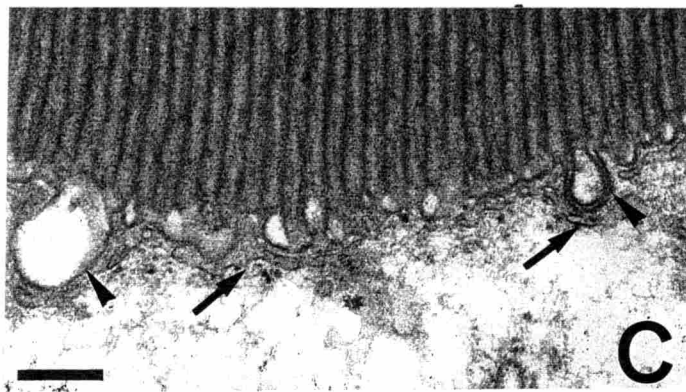
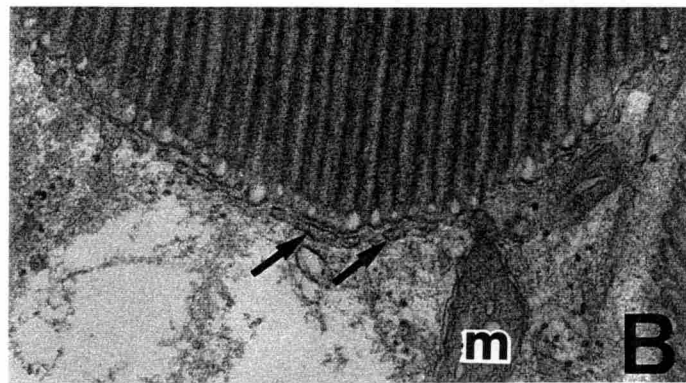
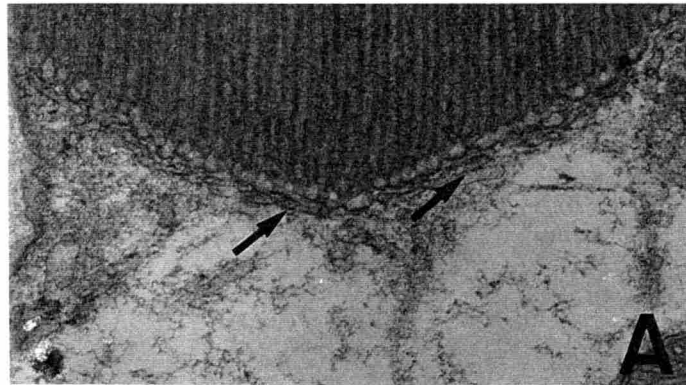


Figure 4. Light-enhanced photoreceptor degeneration in *ninaE^{N196I}*.

Electron micrographs of the transverse sections of ommatidia in the wild-type (**G-I**) and *ninaE^{N196I}* flies (**A-F**). Dark-reared flies (1 day after eclosion) (**A and G**) were put under the constant light for 6 h (**B**), 12 h (**C**), 24 h (**D**), 48 h (**E and H**) and 96 h (**F and I**).

(**A-F**, *ninaE^{N196I}*)

A, 0 h. Intact but a little smaller rhabdomeres are observed. *Arrowheads* indicate zonula adhesions.

B, 6 h. The basal border of rhabdomeres are disorganized.

C, 12h. The size of rhabdomere is evidently decrease . Many aberrant membranes appear in the cytoplasm. Photoreceptor cells look electron-dense.

D, 24 h. Rhabdomeres are remarkably disrupted. Many vacuoles emerge in the cytoplasm. *Arrowheads* indicate the release of membranous sacs to the intraommatidial space.

E, 48 h. Only remnant and short microvilli are observed in the rhabdomeric regions. Photoreceptor cells are swelling. *Arrowheads* indicate the release of the membranous sacs to the intraommatidial space.

F, 96 h. Photoreceptor cells are largely vacuolated and get to be swollen (*large arrow*). Some cells are shrinking (*small arrows*). Zonula adhesions are missing and the second pigment cells intrude between the photoreceptor cells (*arrowheads*).

(**G-I** , wild-type)

G, 0 h.

H, 48 h. Almost intact rhabdomeres like in **G**.

I , 96 h. Rhabdomeres are slightly disorganized, but much less severe than those in *ninaE^{N196I}* flies.

The position of the R7 photoreceptor cells is indicated by *asterisk* in **A** representatively. Note that R7 cells are intact even in the degenerating mutant retinae. *Scale Bar*: 1 μ m

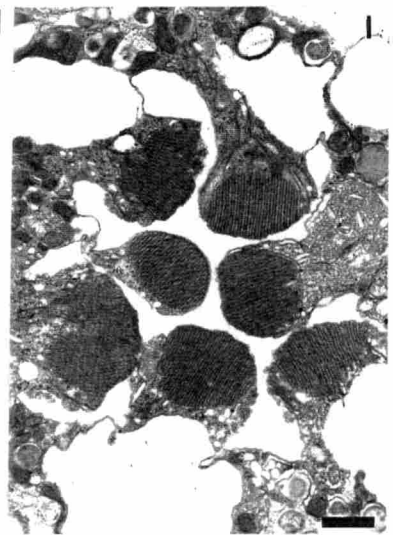
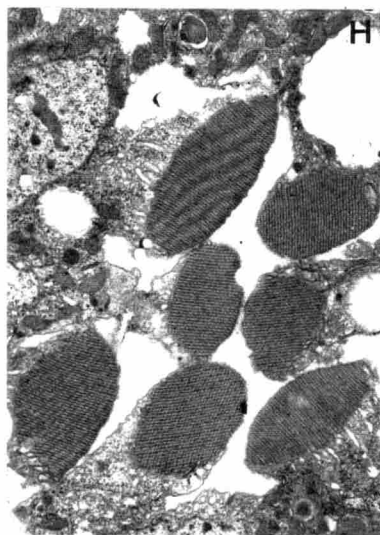
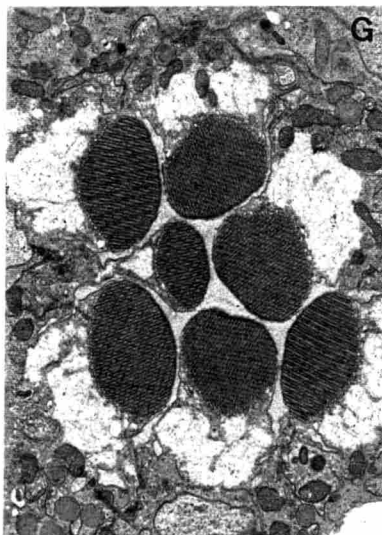
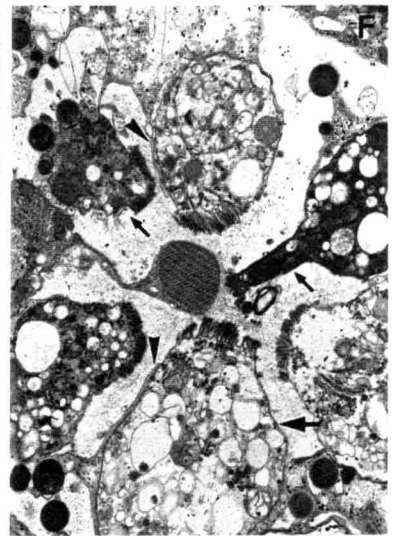
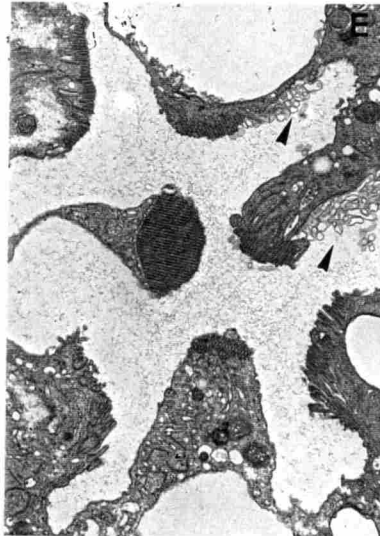
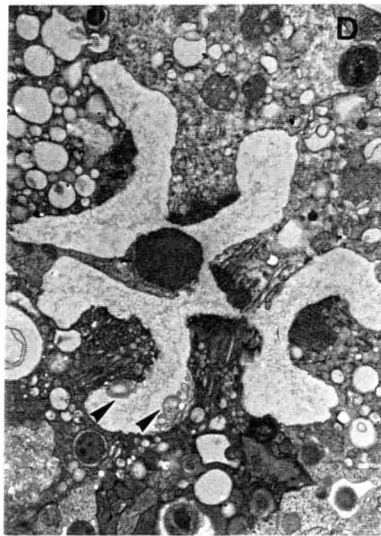
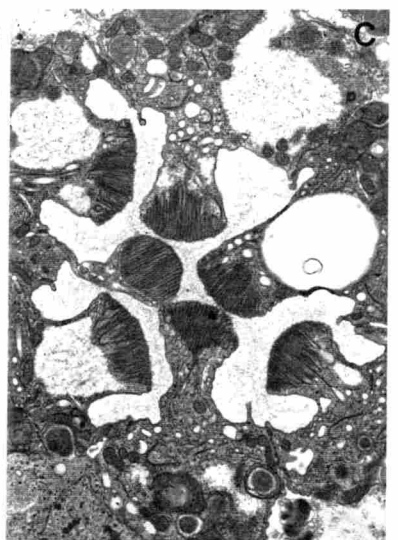
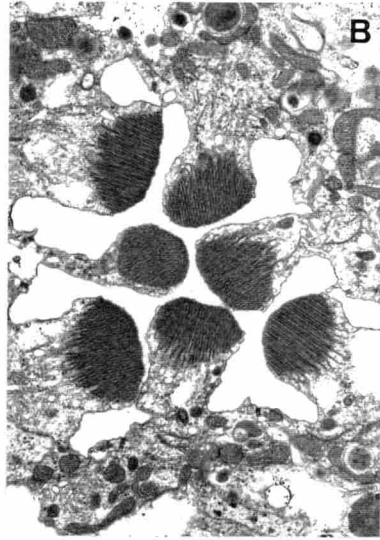
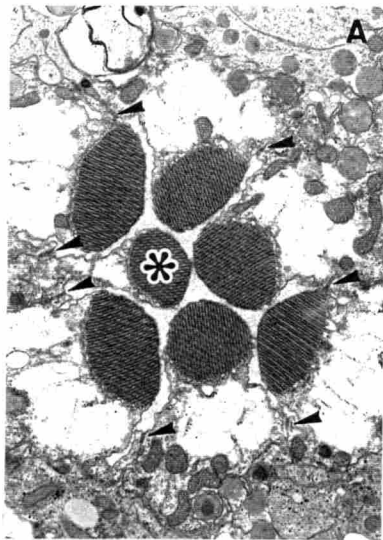


Figure 5. High magnification views of the degenerating photoreceptor cells in the light.

Electron micrographs of the rhabdomeres and cell bodies of *ninaE* *N196I* photoreceptors 1-12 h after light-on.

A and B, 1 h after light-on. Rhabdomeric microvilli invaginate into cytoplasm. *Arrow* indicates one of loop-like membrane structures. *Arrowheads* indicate swollen ends of invagination.

C, 3 h after light-on. The membranes are invaginated deep into the cell body.

D, 6 h after light-on. Invaginations are swollen extensively (*arrow*).

E, 24 h after light-on. Invaginations are swollen much extensively (*arrow*).

Small arrowheads, rERs; N, nucleus ; Scale Bar: 250 nm

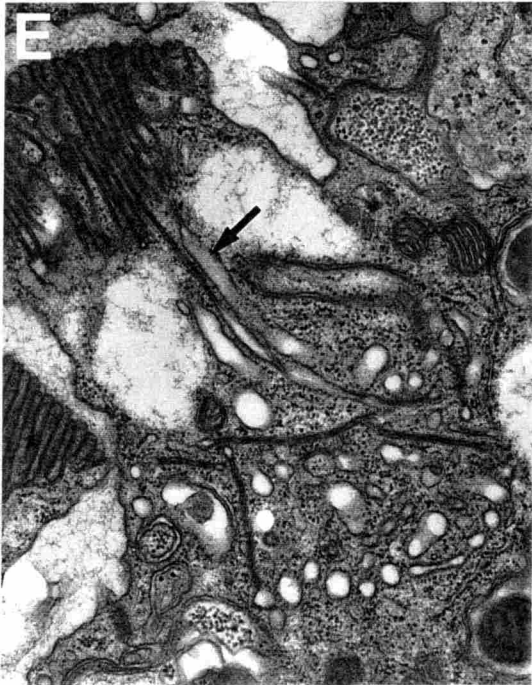
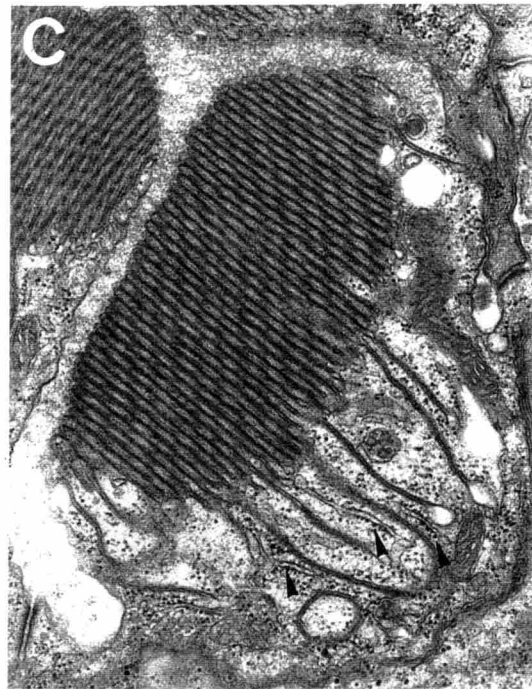
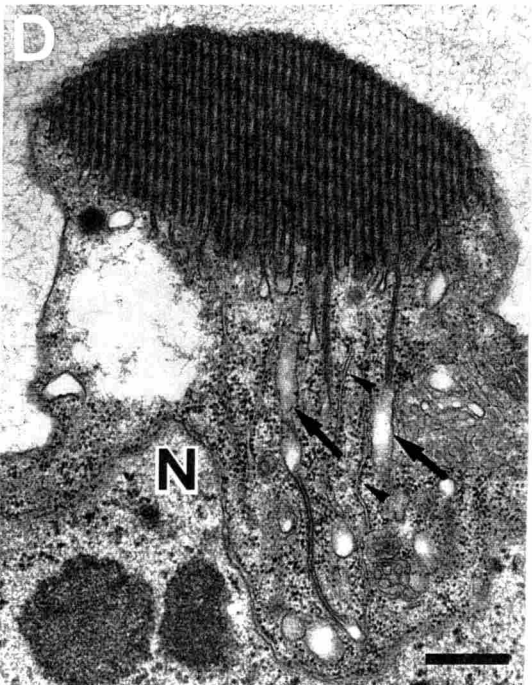
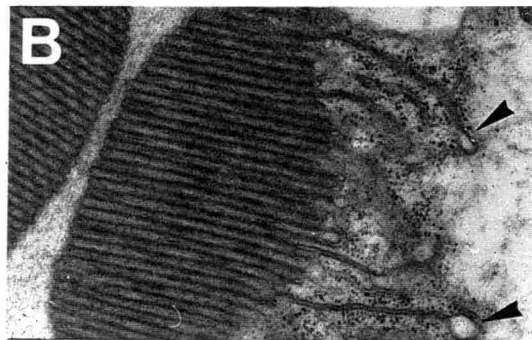
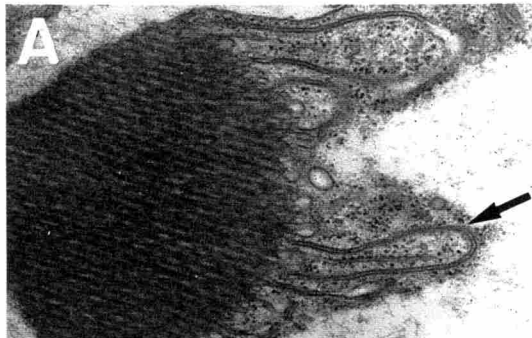


Figure 6. Massive accumulation of the membranous sacs in the degenerating photoreceptors.

Electron micrographs of remnant rhabdomeres (**A and B**) and stalk portion (**C and D**) of the *ninaE*^{N196I} photoreceptor cells 24-48 h after light-on.

A, Membrane accumulation at the remnant rhabdomere region. A sac open to the intraommatidial space (*arrowhead*).

B, Sacs are released from the top of the rhabdomere to the intraommatidial space.

C, Membrane accumulation underneath the rhabdomere.

D, The accumulated sacs, maybe as shown in **C**, are released from the lateral membrane of the stalk to the intraommatidial space. The release from this position is often observed (see also Figure 4D, E).

Asterisks, remnant rhabdomeres; *arrow*, mitochondria; *N*, nucleus ;

Scale Bar: 500 nm

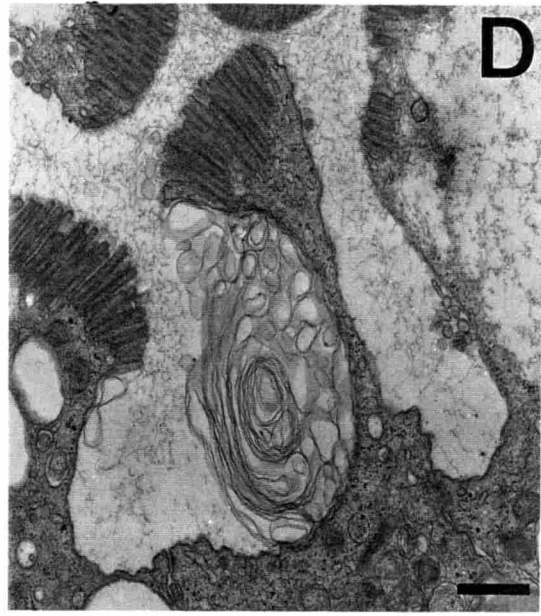
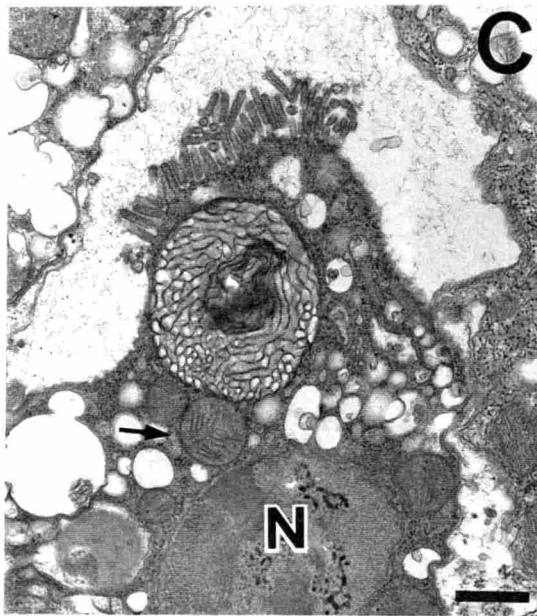
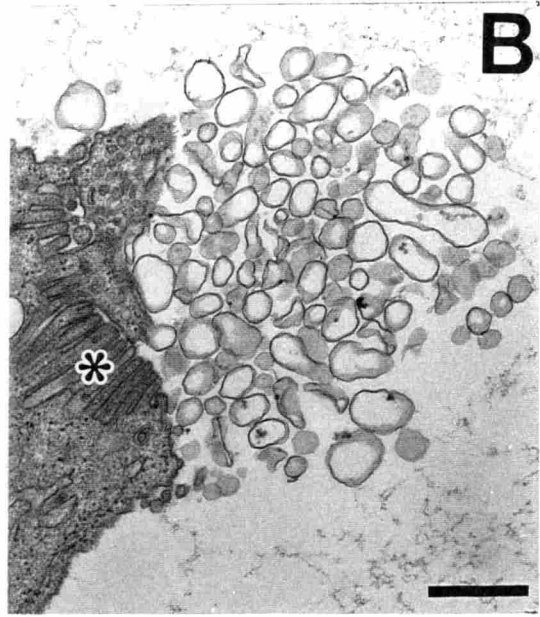
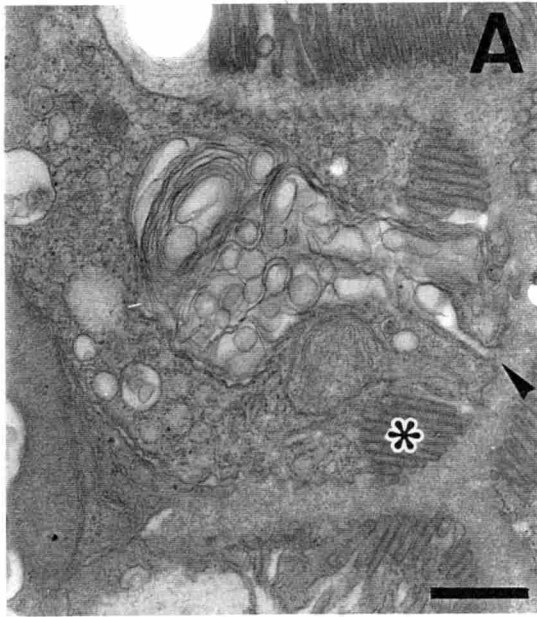


Figure 7. Subcellular localization of the mutant opsin in the *ninaE^{N196I}* photoreceptor cells.

Immunocytochemical localization of the mutant opsin in the *ninaE^{N196I}* photoreceptor cells was examined with anti-rhodopsin antibody (MAb) and immunogold-staining. The flies were reared in the dark and used 0 day after eclosion.

A, Rhabdom of *ninaE^{N196I}* mutant. Gold particles are observed exclusively on the rhabdomeral membranes.

B, One of the peripheral photoreceptor cells (R1-6) of *ninaE^{N196I}* mutant. Only a few gold particles are observed in the cell body.

Asterisks, R7 photoreceptor cell; Scale Bar: 500 nm

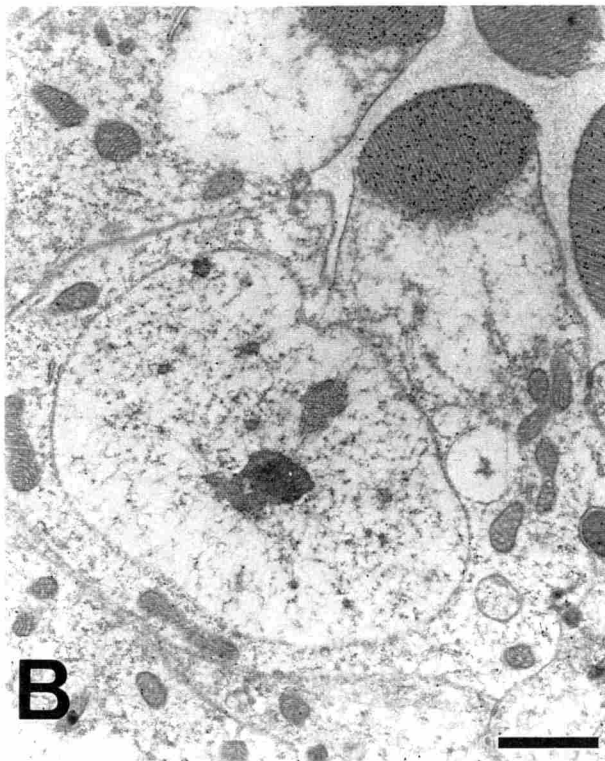


Figure 8. Subcellular localization of the mutant opsin in the degenerating photoreceptor cells.

Immunocytochemical localization of the mutant opsin in the *ninaE* *N196I* photoreceptor cells was examined with polyclonal anti-rhodopsin antibody (PAb) and immunogold-staining. Dark-reared flies (1 day after eclosion) were exposed to the light for 24-48 h.

Gold particles are localized on the various membranous structures.

A and B, Membrane invaginations and sacs beneath the rhabdomere (top) are immunolabeled.

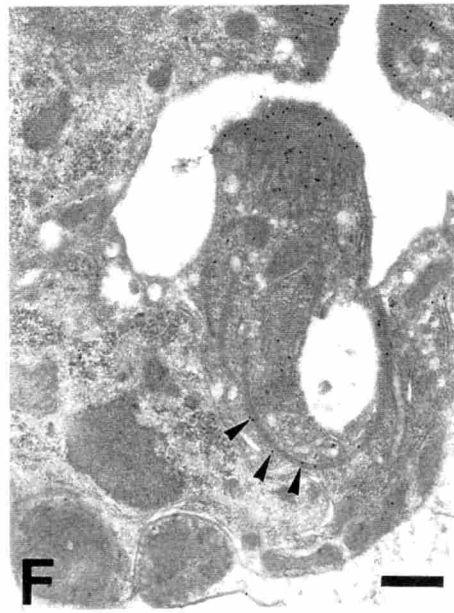
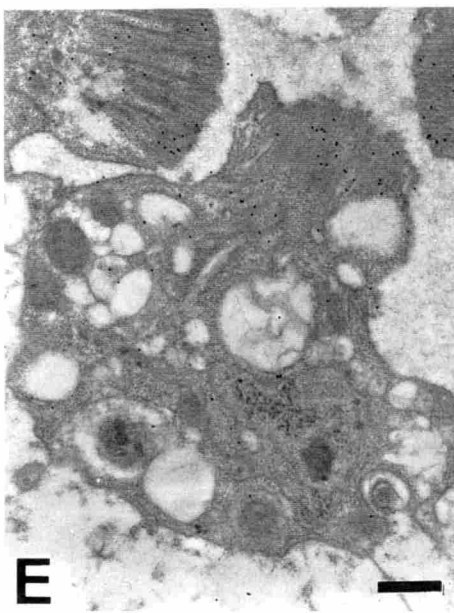
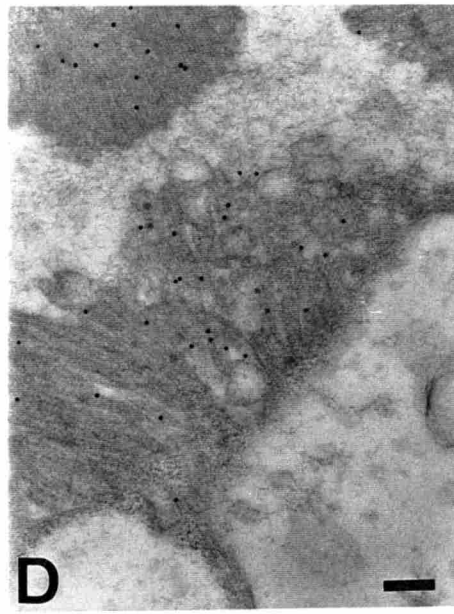
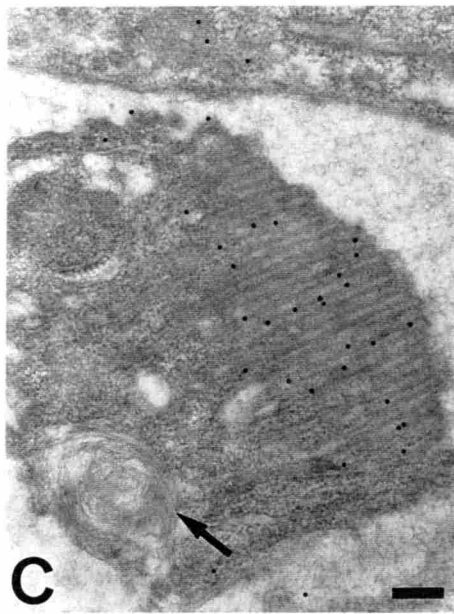
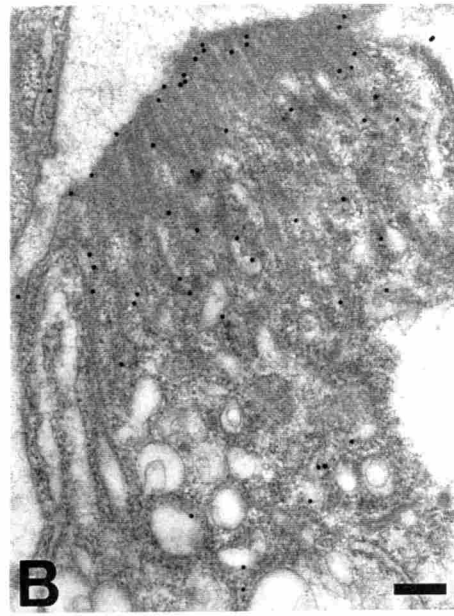
C, Lamellar membranous structure in the cell body is not immunolabeled (*Arrow*).

D, Immunolabeled membranes are released to the extracellular space.

E, Gold particles are found on the vacuoles in the cell body.

F, Gold particles are observed along deeply intruded membranes in the cell body.

Scale Bar: 200 nm in **A-D**, 500 nm in **E** and **F**.



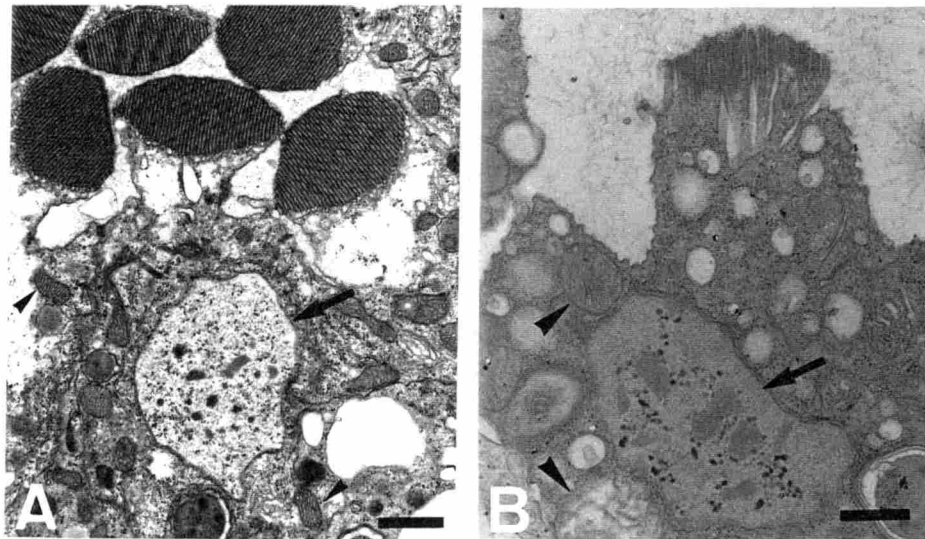


Figure 9. Aberrant feature of nucleus and mitochondria in the degenerating *ninaE*^{N196} photoreceptor cells.

A Dark-reared *ninaE*^{N196I} (0 day after eclosion). Nucleus (*arrow*) and mitochondria (*arrowhead*) are normal.

B Dark-reared *ninaE*^{N196I} were subsequently exposed to the constant light for 24 h. Electron-dense particles emerge in the nucleus (*arrow*). Mitochondria swell out and become round-shaped (*arrowhead*).

Scale Bar: 250 nm in **A**, 500 nm in **B**

Figure 10. Time course of the light-enhanced degradation of opsin in wild-type and *ninaE^{N196I}* flies.

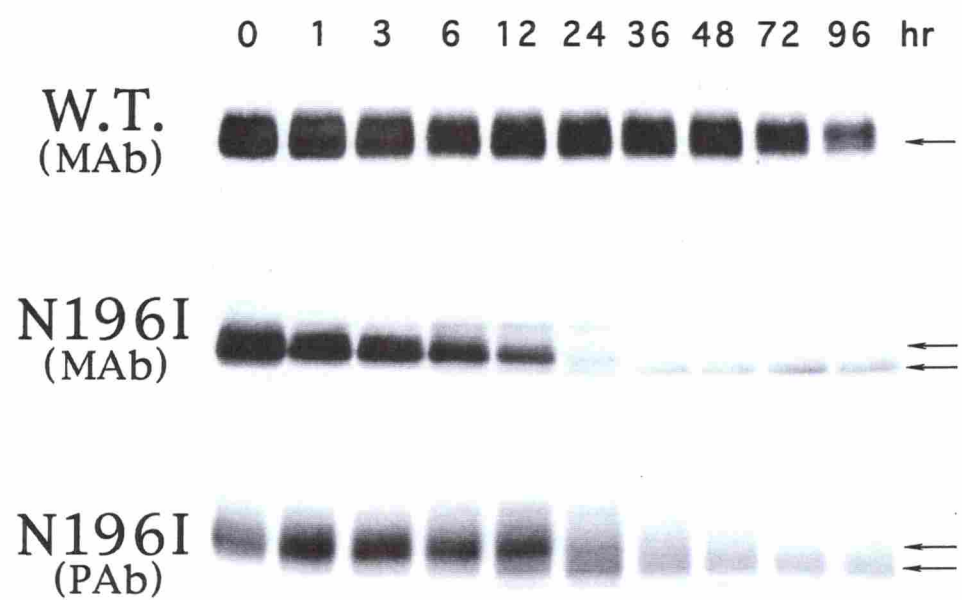
Immunoblot analysis of opsin degradation in the light-exposed wild-type and *ninaE^{N196I}* flies. Dark-reared flies (0-1 day after eclosion) were exposed to the constant light for indicated periods (numbers at the top of the lane, hours). Retinal membrane proteins of the flies were electrophoretically separated and transblotted onto the PVDF membranes, which are subsequently incubated with monoclonal (MAb) or polyclonal (PAb) anti-rhodopsin antibodies. Each lane contains the extract from 1 eye in A, 5 eyes in B and 2 eyes in C.

A, The blot of wild-type was probed with MAb. Mature opsin is degraded after long exposure to the light (48-96 h) .

B, The blot of *ninaE^{N196I}* was probed with MAb. Mature opsin is rapidly degraded as a function of time.

C, The blot of *ninaE^{N196I}* was probed with PAb. PAb shows higher immunoreactivity against the degraded opsin than MAb.

Solid circles, mature opsin; *Solid triangles*, degraded opsin



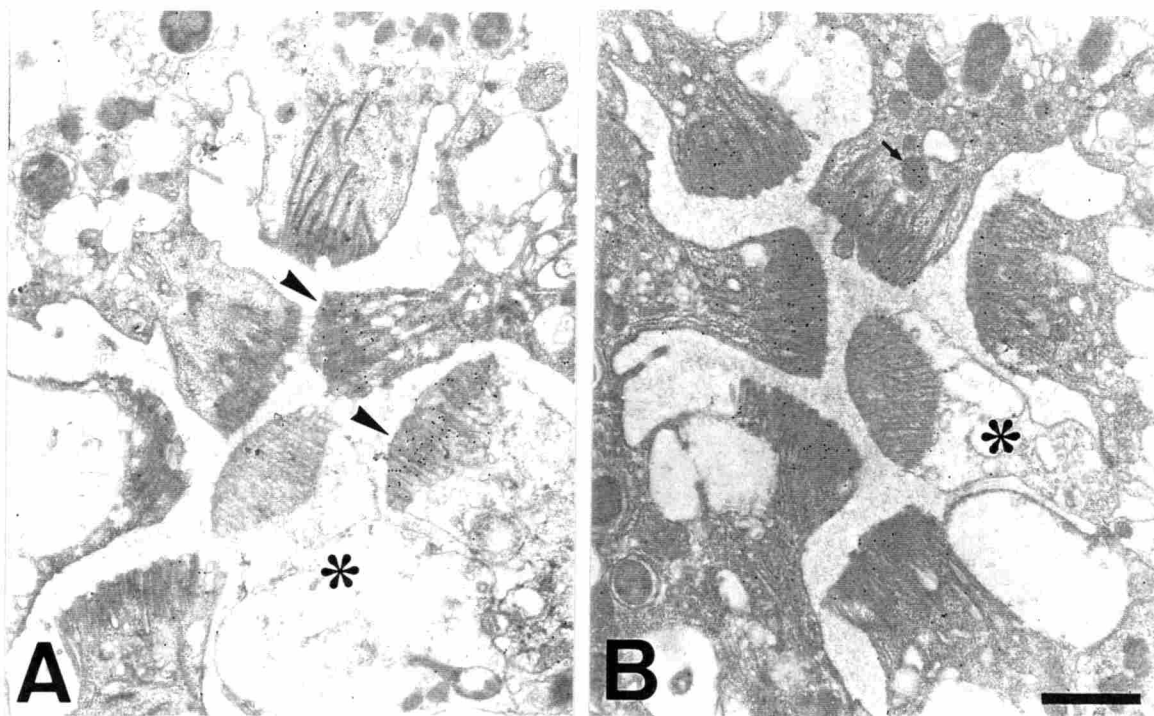


Figure 11. Subcellular distribution of degraded opsin in the degenerating photoreceptor cells of *ninaE*^{N196I}.

Immunocytochemical localization of the degraded opsin was examined with two kinds of anti-rhodopsin antibodies, MAb and PAb. Dark-reared *ninaE*^{N196I} mutant (1 day after eclosion) were exposed to the constant light for 48 h. Transverse sections from a single eye were probed with MAb (A) or PAb (B).

A, MAb-directed gold particles are restrictedly distributed on a few rhabdomeres in a single ommatidium. Gold particles are also found in the cell bodies.

B, PAb-directed gold particles are observed in all rhabdomeres examined. Some gold particles are also found in the cell bodies. *Small arrow* indicates a multivesicular body (MVB), which is stained with gold particles, too.

Asterisks, R7 photoreceptor cell; Scale Bar: 1 μm

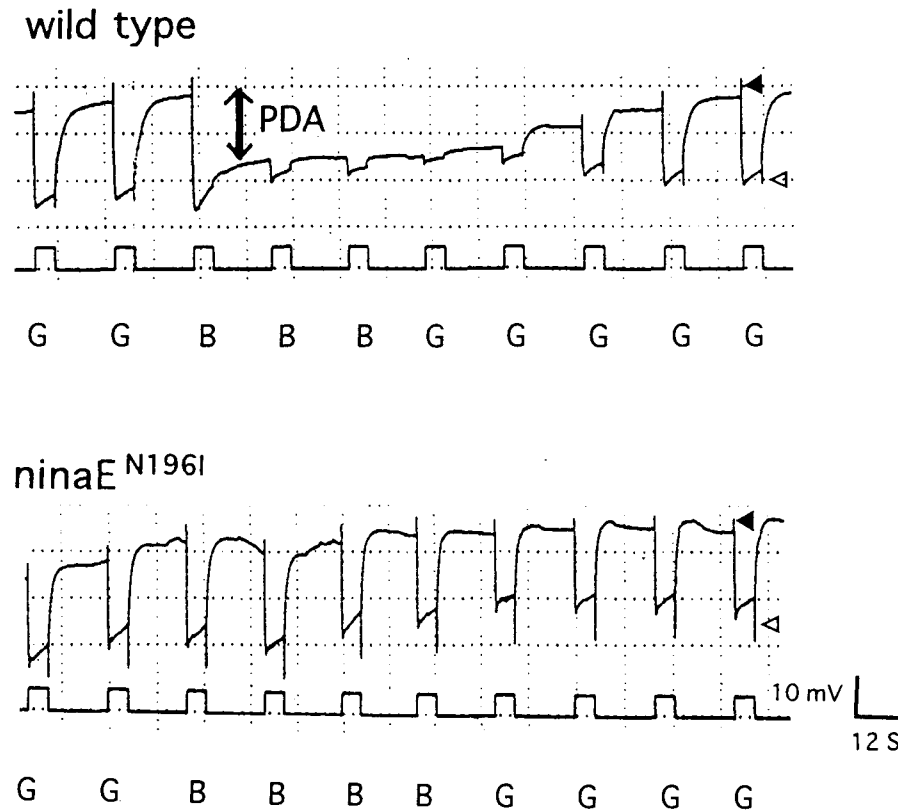


Figure 12. Electrophoretograms of wild-type and *ninaE*^{N196I} mutant.

ERGs of the young wild-type and *ninaE*^{N196I} mutant flies reared in the constant darkness (0-2 days after eclosion). The stimulus (bottom trace in each panel) consists of a series of ten 5s light pulses; G, green; B, blue. *ninaE*^{N196I} mutant shows normal ERG phenotype except absence of PDA, the prolonged depolarizing afterpotential.

Solid triangles, on-transients; open triangles, off-transients

Figure 13. Opsin levels in the heterozygous *ninaE* mutants.

Immunoblot analysis of opsin contents in the wild-type and several *ninaE* heterozygotes. Flies were reared in the 12L/12D light cycle and used 0-2 days after eclosion. Retinal membrane proteins of the flies were electrophoretically separated and transblotted onto the PVDF membranes, which were subsequently incubated with anti-rhodopsin antibodies (MAb). Each lane contains the extract from 2 eyes.

lane 1, Wild type (+ / +).

lane 2, *ninaE*^{*oI17*} / + heterozygote. The opsin level is slightly reduced compared with that of wild-type (*lane 1*). *ninaE*^{*oI17*} is a null mutant allele.

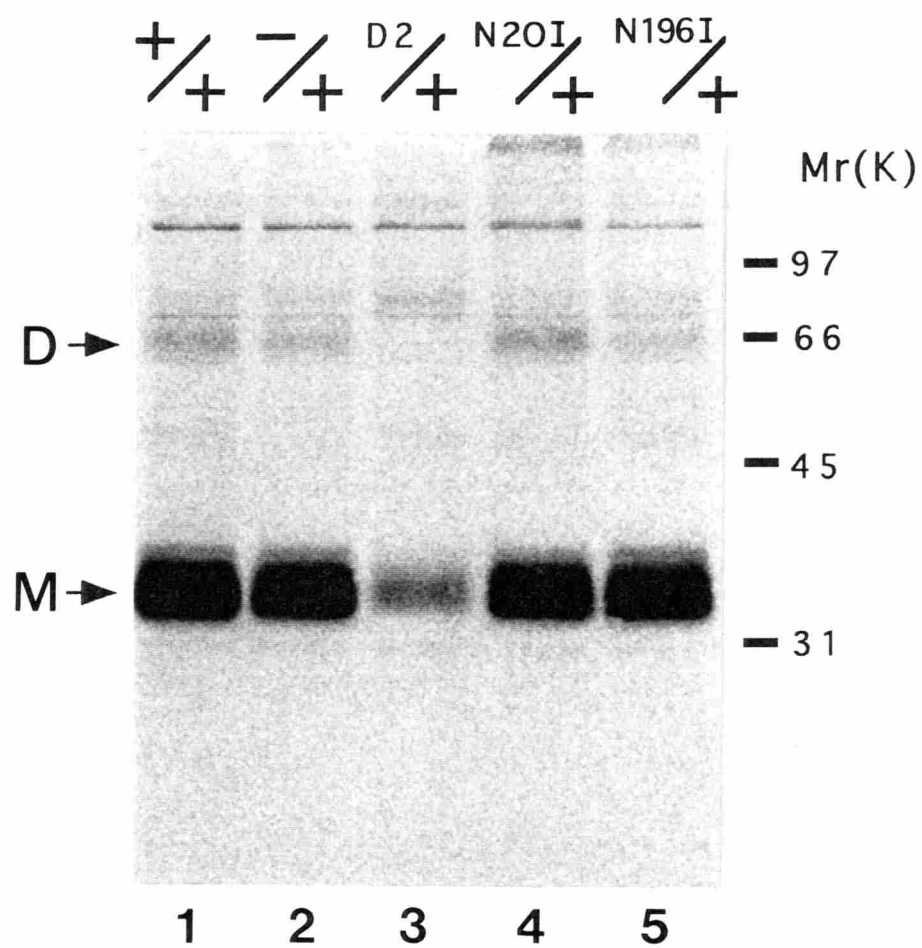
lane 3, *ninaE*^{*D2*} / + heterozygote. Opsin is remarkably reduced, because *ninaE*^{*D2*} is a dominant mutant allele.

lane 4. *ninaE*^{*N20I*} / + heterozygote. The opsin level is comparable to that of *ninaE*^{*oI17*} / + (*lane 2*). *ninaE*^{*N20I*} is a mutant allele that causes a loss of N-glycosylation of opsin.

lane 5. *ninaE*^{*N196I*} / + heterozygote. The opsin level is comparable to that of *ninaE*^{*oI17*} / + (*lane 2*), indicating that the *ninaE*^{*N196I*} allele is recessive for wild-type.

M, monomer of mature opsin; D, Dimmer of mature opsin.

The numbers on the right side indicate molecular size markers (k).



References

Applebury, M.L. and Hargrave, P.A. (1986). Molecular biology of the visual pigments. *Vision Res.* 26, 1881-1895.

Baker, E. K., Colley, N. J. and Zuker, C. S. (1994). The cyclophilin homolog NinaA functions as a chaperone, forming a stable complex *in vivo* with its protein target rhodopsin. *EMBO J.* 13, 4886-4895.

Bentrop, J., Schwab, K., Pak, W. L. and Paulsen, R. (1997). Site-directed mutagenesis of highly conserved amino acids in the first cytoplasmic loop of *Drosophila* Rh1 opsin blocks rhodopsin synthesis in the nascent state. *EMBO J.* 16, 1600-1609.

Brown, G., Chen, D. -M., Christianson, J. S., Lee, R. and Stark, W. S. (1994). Receptor demise from alteration of glycosylation site in *Drosophila* opsin: Electrophysiology, microspectrophotometry, and electron microscopy. *Vis. Neurosci.* 11, 619-628.

Cailliau, C. P., Sung, C.-H., Nathans, J. and Adler, R. (1993). Apoptotic photoreceptor cell death in mouse models of retinitis pigmentosa. *Proc. Natl. Acad. Sci. USA.* 91, 974-978.

Chang, G.-Q., Hao, Y. and Wong, F. (1993). Apoptosis: Final common pathway of photoreceptor death in *rd*, *rds*, and rhodopsin mutant mice. *Neuron* 11, 595-605.

Chirgwin, J. M., Przybyla, A. E., MacDonald, R. J. and Rutter, W. J. (1979). Isolation of biologically active ribonucleic acid from sources enriched in ribonuclease. *Biochemistry* 18, 5294-5299.

Colley, N. J., Baker, E. K., Stamnes, M. A. and Zuker, C. S. (1991). The cyclophilin homolog ninaA is required in the secretory pathway. *Cell* 67, 255-263.

Colley, N. J., Cassill J. A., Baker, E. K. and Zuker, C. S. (1995). Defective intracellular transport is the molecular basis of rhodopsin-dependent dominant retinal degeneration. *Proc. Natl. Acad. Sci. USA* 92, 3070-3074.

De Couet, H. G. and Tanimura, T. (1987). Monoclonal antibodies provide evidence that rhodopsin in the outer rhabdomeres of *Drosophila melanogaster* is not glycosylated. *Eur. J. Cell Biol.* 44, 50-56.

Doi, T., Molday, R. S. and Khorana, H. G. (1990). Role of the intradiscal domain in rhodopsin assembly and function. *Proc. Natl. Acad. Sci. USA* 87, 4991-4995.

Dryja, T. P., McGee, T. L., Reichel, E., Hahn, L. B., Cowley, G. S. Yandell, D. W., Sandberg, M. A. and Berson E. L. (1990). A point mutation of the rhodopsin gene in one form of retinitis pigmentosa. *Nature* 343,364-366.

Dryja, T. P., Berson, E. L., Rao, V. R. and Oprian, D. D. (1993). Heterozygous missense mutation in the rhodopsin gene as a cause of congenital stationary night blindness. *Nature Genet.* 4, 280-283.

Duffin, K. L., Lange, G. W., Welply, J. K., Florman, R., O'Brien, P. J., Dell, A., Reason, A. J., Morris, H. R. and Fliesler, S. J. (1993). Identification and oligosaccharide structure analysis of rhodopsin glycoforms containing galactose and sialic acid. *Glycobiol.* 3, 365-380.

Farber, D. B. and Danciger, M. (1997). Identification of genes causing photoreceptor degenerations leading to blindness. *Curr. Opin. Neurobiol.* 7, 666-673.

Ferreira, P. A., Nakayama, T. A., Pak, W. L. and Travis, G. H. (1996). Cyclophilin-related protein RanBP2 acts as chaperone for red/green opsin. *Nature* 383, 637-640.

Fiedler, K. and Simons, K. (1995). The role of N-glycans in the secretory pathway. *Cell* 81, 309-312.

Fliesler, S. J., Rapp, L. M. and Hollyfield, J. G. (1984)..Photoreceptor-specific degeneration caused by tunicamycin. *Nature* 311, 575-577.

Fliesler, S. J. and Basinger, S. F. (1985). Tunicamycin blocks the incorporation of opsin into retinal rod outer segment membranes. *Proc. Natl. Acad. Sci. USA* 82, 1116-1120.

Fliesler, S. J., Rayborn, M. E. and Hollyfield, J. G. (1985). Membrane morphogenesis in retinal rod outer segments: Inhibition by tunicamycin. *J. Cell Biol.* 100, 574-587.

Gal A., Apfelstedt-Sylla E., Janecke A. R. and Zrenner E. (1997). Rhodopsin mutation in inherited retinal dystrophies and dysfunctions. *Progress in Retinal and Eye Research* 16, 51-79.

Hargrave, P. A. (1977). The amino-terminal tryptic peptide of bovine rhodopsin: a glycopeptide containing two sites of oligosaccharide attachment. *Biochim. Biophys. Acta* 492, 83-94.

- Hebert, D. N., Foellmer, B. and Helenius, A. (1995). Glucose trimming and reglucosylation determine glycoprotein association with calnexin in the endoplasmic reticulum. *Cell* 81, 425-433.
- Helenius, A. (1994). How N-linked oligosaccharides affect glycoprotein folding in the endoplasmic reticulum. *Mol. Biol. Cell* 5, 253-265.
- Huber, A., Smith, D. P., Zuker, C. S. and Paulsen, R. (1990). Opsin of *Calliphora* peripheral photoreceptors R1-6: Homology with *Drosophila* Rh1 and post-translational processing. *J. Biol. Chem.* 265, 17906-17910.
- Huber, A., Wolfrum, U. and Paulsen, R. (1993). Opsin maturation and targeting to rhabdomeral photoreceptor membranes requires the retinal chromophore. *Eur. J. Cell Biol.* 63, 219-229.
- Humphries, M. M., Rancourt, D., Farrar, G. J., Kenna, P., Hazel, M., Bush, R. A., Sieving, P. A., Sheils, D. M., McNally, N., Creighton, P. Erven, A., Boros, A., Gulya, K., Capecchi, M. R. and Humphries, P. (1997). Retinopathy induced in mice by targeted disruption of the rhodopsin gene. *Nature Genet.* [letter] 15, 216-219.
- Johnson, E. C. and Pak, W. L. (1986). Electrophysiological study of *Drosophila* rhodopsin mutants. *J. Gen. Physiol.* 651-673.
- Ju, J., Fujita, S., Endo, T., Kobata, A. and Kean, E. L. (1994). The oligosaccharide chains of human rhodopsin. *Invest. Ophthalmol. Vis. Sci.* 35 (Suppl), 1460.
- Karnik, S. S. and Khorana, H. G. (1990). Assembly of functional rhodopsin requires a disulfide bond between cysteine residues 110 and 187. *J. Biol. Chem.* 265, 17520-17524.
- Kaushal, S. and Khorana, H. G. (1994) Structure and function in rhodopsin. 7. Point mutations associated with autosomal dominant retinitis pigmentosa. *Biochemistry* 33, 6121-6128.
- Kaushal, S., Ridge, K. D. and Khorana, H. G. (1994). Structure and function in rhodopsin: The role of asparagine-linked glycosylation. *Proc. Natl. Acad. Sci. USA* 91, 4024-4028.
- Keen, T. J., Inglehearn, C. F., Lester, D. H., Bashir, R., Jay, M., Bird, A. C., Jay, B. and Bhattacharya, S. S. (1991). Autosomal dominant retinitis pigmentosa: four new mutations in rhodopsin, one of them in the retinal attachment site. *Genomics* 11, 199-205.

- Kornfeld, R. and Kornfeld, S. (1985). Assembly of asparagine-linked oligosaccharides. *Ann. Rev. Biochem.* 54, 631-664.
- Kumar, J. P. and Ready, D. (1995). Rhodopsin plays an essential structural role in *Drosophila* photoreceptor development. *Development* 121, 4359-4370.
- Kumaramanickavel, G., Maw, M., Denton, M. J., John, S., Srikumari., C. R., Orth, U. Oehlmann, R. and Gal, A. (1994). Missense rhodopsin mutation in a family with recessive RP. *Nature Genet.* [letter] 8, 10-11.
- Kurada, P. and O'Tousa, J.E. (1995). Retinal degeneration caused by dominant rhodopsin mutations in *Drosophila*. *Neuron* 14, 571-579.
- Laemmli, U. K. (1970). Cleavage of structural proteins during the assembly of the head of the bacteriophage T4. *Nature* 227, 680-685.
- Leonard, D. S., Bowman, V. D., Ready, D. F. and Pak, W. L. (1992). Degeneration of photoreceptors in rhodopsin mutants of *Drosophila*. *J. Neurobiol.* 23, 605-626.
- Li, T., Franson W. K., Gordon J. W., Berson E. L. and Dryja, T. P. (1995). Constitutive activation of phototransduction by K296E opsin is not a cause of photoreceptor degeneration. *Proc. Natl. Acad. Sci. USA.* 92, 3551-3555.
- Lis, H. and Sharon, N. (1993). Protein glycosylation: structural and functional aspects. *Eur. J. Biochem.* 218, 1-27.
- Marshall, R.D. (1972). Glycoproteins. *Ann. Rev. Biochem.* 41, 673-702.
- Matsumoto-Suzuki, E., Hirosawa, K. and Hotta, Y. (1989). Structure of the subrhabdomeric cisternae in the photoreceptor cells of *Drosophila melanogaster*. *J. Neurocytol.* 18, 87-93.
- Min K. C., Zvyaga T. A., Cypress A. M. and Sakmer T. P. (1993). Characterization of mutant rhodopsin responsible for autosomal dominant retinitis pigmentosa; mutation on cytoplasmic surface affect transducin activation. *J. Biol. Chem.* 268, 9400-9404.
- Nashima, K., Mitsudo, M. and Kito, Y. (1978). Studies on Cephalopod rhodopsin: fatty acid esters of sucrose as effective detergents. *Biochim. Biophys. Acta* 536, 78-87.
- Okano, T., Kojima, D., Fukada, Y., Shichida, Y. and Yoshizawa, T. (1992). Primary structures of chicken cone visual pigments: Vertebrate rhodopsins have evolved out of cone visual pigments. *Proc. Natl. Acad. Sci. USA* 89, 5932-5936.

O'Tousa, J. E., Baehr, W., Martin, R. L., Hirsh, J., Pak, W. L. and Applebury, M. L. (1985). The *Drosophila ninaE* gene encodes an opsin. *Cell* 40, 839-850.

O'Tousa, J. E., Leonard, D. S. and Pak, W. L. (1989). Morphological defects in *ora^{JK84}* photoreceptors caused by mutation in R1-6 opsin gene of *Drosophila*. *J. Neurosci.* 6, 41-52.

O'Tousa, J. E. (1992). Requirement of N-linked glycosylation site in *Drosophila* rhodopsin. *Vis. Neurosci.* 8, 385-390.

Ou, W. -J., Cameron, P. H., Thomas, D. Y. and Bergeron, J. J. (1993). Association of folding intermediates of glycoproteins with calnexin during protein maturation. *Nature* 364, 771-776.

Ozaki, K., Nagatani, H., Ozaki, M. and Tokunaga, F. (1993). Maturation of major *Drosophila* rhodopsin, *ninaE*, requires chromophore 3-hydroxyretinal. *Neuron* 10, 1113-1119.

Peterson, J. R., Ora, A., Van, P. N. and Helenius, A. (1995). Transient, lectin-like association of calreticulin with folding intermediates of cellular and viral glycoproteins. *Mol. Biol. Cell* 6, 1173-1184.

Plantner, J. J., Poncz, L. and Kean, E. L. (1980). Effect of tunicamycin on the glycosylation of rhodopsin. *Arch. Biochem. Biophys.* 201, 527-532.

Rao, V. R., Cohen, G. B. and Oprian, D. D. (1994). Rhodopsin mutation G90D and a molecular mechanism for congenital night blindness. *Nature* 367, 639-642.

Richards, J. E., Scott, K. M. and Sieving, P. A. (1994). Disruption of conserved rhodopsin disulfide bond by Cys187Tyr mutation causes early and severe autosomal dominant retinitis pigmentosa. *Ophthalmology* 102, 669-677.

Ridge, K. D., Lu, Z., Liu, X. and Khorana, H. G. (1995). Structure and function in rhodopsin. Separation and characterization of the correctly folded and misfolded opsin produced on expression of an opsin mutant gene containing only the native intradiscal cysteine codons. *Biochemistry* 34, 3261-3267.

Robinson, P. R., Cohen, G. B., Zhukovsky, E. A., and Oprian, D. D. (1992). Constitutively active mutants of rhodopsin. *Neuron* 9, 719-725.

Rosenfeld, P. J., Cowley, G. S., McGee, T. L., Sandberg, M. A., Berson, E. L. and Dryja, T. P. (1992). A null mutation in the rhodopsin gene causes rod photoreceptor dysfunction and autosomal recessive retinitis pigmentosa. *Nat. Genet.* 1, 209-213.

Sanger, F., Nicklen, S., and Coulson, A. R. (1977). DNA sequencing with chain-terminating inhibitors. *Proc Natl Acad Sci U S A* 74, 5463-5467

Sapp, R. J., Christianson, J. S., Maier, L., Studer, K. and Stark, W.S. (1991a). Carotenoid replacement therapy in *Drosophila*: Recovery of membrane, opsin and visual pigment. *Exp. Eye Res.* 53, 73-79.

Sapp, R. J., Christianson, J. S. and Stark, W.S. (1991b). Turnover of membrane and opsin in visual receptors of normal and mutant *Drosophila*. *J. Neurocytol.* 20, 597-608.

Satoh, A. K., Tokunaga, F., Kawamura, S. and Ozaki, K. (1997). In situ inhibition of vesicle transport and protein processing in the dominant negative Rab1 mutant of *Drosophila*. *J. Cell Sci.* 2943-2953.

Scavarda, N.J., O'Tousa, J.E. and Pak, W.L. (1983). *Drosophila* locus with gene-dosage effects on rhodopsin. *Proc. Natl. Acad. Sci. USA* 80, 4441-4445.

Schneuwly, S., Shortridge, R. D., Larrivee, D. C., Ono, T., Ozaki, M. and Pak, W. L. (1989). *Drosophila ninaA* gene encodes an eye-specific cyclophilin (cyclosporine A binding protein). *Proc. Natl. Acad. Sci. USA* 86, 5390-5394.

Shieh, B. -H., Stamnes, M. A., Seavello, S., Harris, G. L. and Zuker, C. S. (1989). The *ninaA* gene required for visual transduction in *Drosophila* encodes a homologue of cyclosporin A-binding protein. *Nature* 338, 67-70.

Smith, W. C., Price, D. A., Greenberg, R. M. and Battelle, B. -A. (1993). Opsins from the lateral eyes and ocelli of the horseshoe crab, *limulus polyphemus*. *Proc. Natl. Acad. Sci. USA* 90, 6150-6154.

Stamnes, M. A., Shieh, B. H., Chuman, L. Harris, G. L., and Zuker, C. S. (1991). The cyclophilin homolog *ninaA* is a tissue-specific integral membrane protein required for the proper synthesis of a subset of *Drosophila* rhodopsins. *Cell* 65, 219-227.

Stark, W. S., Sapp, R. and Schilly, D. (1988). Rhabdomere turnover and rhodopsin cycle: maintenance of retinula cells in *Drosophila melanogaster*. *J. Neurocytol.* 17, 499-509.

Stark, W. S., Christianson, J. S., Maier, L. and Chen, D. -M. (1991). Inherited and environmentally induced retinal degenerations in *Drosophila*. In *Proceedings of the Stockholm Symposium on Retinal Degeneration*, Ed. Anderson, R. E., Hollyfield, J. G., and La Vail, M. M., pp. 61-75. Boca Raton, Florida: CRC Press.

- Steel, F. and O'Tousa, J. E. (1990). Rhodopsin activation causes retinal degeneration in *Drosophila rdgC* mutant. *Neuron* 4, 883-890.
- Sung, C.-H., Schneider, B. G., Agarwal, N., Papermaster, D. S. and Nathans, J. (1991). Functional heterogeneity of mutant rhodopsins responsible for autosomal dominant retinitis pigmentosa. *Proc. Natl. Acad. Sci. USA* 88, 8840-8844.
- Sung, C.-H., Davenport, C. M. and Nathans, J. (1993). Rhodopsin mutations responsible for autosomal dominant retinitis pigmentosa; clustering of functional classes along the polypeptide chain. *J. Biol. Chem.* 268, 26645-26649.
- Tamaki, H. and Yamashina, S. (1994). Improved method for post-embedding cytochemistry using reduced osmium and LR White resin. *J. Histochem. Cytochem.* 42, 1285-1293.
- Vinós, J., Jalink, K., Hardy, R. W., Britt, S. G. and Zuker, C. S. (1997). A G protein-coupled receptor phosphatase required for rhodopsin function. *Science* 277, 687-690.
- Zars, T. and Hyde, R. D. (1996). *rdgE*: A novel retinal degeneration mutation in *Drosophila melanogaster*. *Genetics* 144, 127-138.
- Zuker, C. S., Cowman, A. F. and Rubin, G. M. (1985). Isolation and structure of a rhodopsin gene from *D. melanogaster*. *Cell* 40, 851-858.

Abstract
(in Japanese)

論文要旨

ショウジョウバエロドプシンにおける細胞外領域の重要性

【はじめに】

視物質は動物の光感覚を担う光受容タンパク質であり、視細胞の中の特殊化した多重膜構造（光受容膜）上に高密度で局在している。この構造が視細胞の効率的な光受容を可能とし、視覚の高感度を生み出す理由のひとつとなっている。視物質は7回膜貫通型のタンパク質であり、発色団（11シスレチナール）を結合する膜貫通領域および細胞内領域・細胞外領域の3つの領域に分けることができる。これらの各領域および特徴的なアミノ酸残基の機能に関しては、特に脊椎動物の変異視物質を用いて精力的な解析がおこなわれてきた。その結果、細胞内領域の部分欠失の多くが視物質の発現量低下と構造異常を引き起こすことから、この領域は視物質の構造形成にとって重要であると考えられている。一方、視物質の細胞外領域には、特徴的な構造の一つとしてアスパラギン(N-)結合型糖鎖が存在するが、その機能については、まだはっきりとはわかっていない。ショウジョウバエの視物質（ロドプシン）にも糖鎖が結合することが知られている。しかし、その結合は未成熟な合成中間体に限られ、成熟ロドプシンからは糖鎖が検出されない。このことから、糖鎖はロドプシンの最終的な機能に必要なのではなく、ロドプシン合成や細胞内輸送の過程に必要なものであることが予想される。しかしながら、ショウジョウバエのロドプシンに存在する2カ所の糖鎖付加可能部位（Asn20、Asn196）のどちらに糖鎖が結合するのかは知られていない。また、糖鎖がロドプシン合成のどの段階に関与するのかということについても明らかではない。

本研究では、生体内での変異タンパク質の機能解析が可能なキイロショウジョウバエ（*Drosophila melanogaster*）を用いて、まずロドプシンのN-結合型糖鎖の結合部位とロドプシン合成における役割について検討した。その結果、糖鎖はAsn20のみに結合し、ロドプシン成熟過程に関与することを明らかにした。一方、Asn196の変異はAge-dependentかつlight-enhanced typeの網膜変性を引き起こすことを発見し、その変性過程について詳細な形態学的解析と生化学的解析を行った。

【結果と考察】

1. ロドプシンの糖鎖付加部位の決定

ショウジョウバエロドプシンの糖鎖付加部位を同定するために、まず、*in vitro* 翻訳系を用いてオプシン（ロドプシンのアポタンパク質）の合成を行なった。この系で、2つの糖鎖付加候補残基（Asn20とAsn196）の各々をイソロイシンで置換した変異オプシン2種類（N20I、N196I）を合成した結果、共に分子量40Kの糖鎖を持つオプシンが合成された。これら40Kの分子は、それぞれAsn196とAsn20に1本の糖鎖を持つ変異オプシンであると考えられた。しかしながら、この1本の糖鎖はN20Iオプシンに比べてN196Iオプシンの方に付加しやすい傾向がみられた。さらに、この40Kの分子は生体内のオプシン合成中間体と似た分子量を示すことから、生体内の合成中間体はおそらく糖鎖を1本結合しており、その結合部位はAsn20ではないかと考えられた。

これを *in vivo* で確認するため、2種類の形質転換体 *nina E*^{N20I} および *nina E*^{N196I}（それぞれ N20I、N196I 変異オプシンのみを発現）を用いて実験を行なった。野生型のハエをカロチノイド欠乏培地で飼育すると、ロドプシンは成熟せず、糖鎖の付加した分子量40Kの未成熟オプシン（＝合成中間体）のみが蓄積することが知られている。しかし *nina E*^{N20I} では、この条件下でも糖鎖の付加した合成中間体はまったく見られず、代わって糖鎖の付加していない分子量36Kの中間体が観察された。一方、*nina E*^{N196I} では野生型と同様に糖鎖の付加した40K合成中間体が生じていた。以上の結果からショウジョウバエロドプシンの生体内での糖鎖付加位置がAsn20であることが明確に示された。

2. ロドプシン成熟過程における糖鎖の関与

Asn20に付加した糖鎖がロドプシン合成のどの段階で必要であるのかを調べるために合成の各段階での発現量を *ninaE^{N20I}* と *ninaE^{N196I}* および野生型のハエで比較した。その結果、カロチノイド欠乏時の合成中間体については両変異体で量の違いは見られないことがわかった。しかしながら成熟オプシンの量は野生型や *ninaE^{N196I}* に比べて *ninaE^{N20I}* で大きく減少した。以上の結果から、糖鎖は合成中間体より以降の成熟あるいは輸送の過程に関与していることが示された。*ninaE^{N20I}* で微量の成熟オプシンも観察されたことから、糖鎖がなくとも成熟過程は進行可能ではあるが、糖鎖はその効率を大幅に上昇させている可能性が考えられた。

3. 形質転換体 *ninaE^{N196I}* における変異形質の解析

Asn196は糖鎖付加には関与しないにもかかわらず、これを失った *ninaE^{N196I}* のロドプシンの発現量は恒暗条件下で野生型の約20%に減少した。これはAsn196が糖鎖付加とは異なる役割をもつことを示唆している。そこでこの部位の役割を理解するために、光条件を変えてロドプシン量と細胞形態の変化を継時的に観察した。

暗黒下飼育した生後間もない *ninaE^{N196I}* の視細胞は、光受容部位（ラブドメア）が野生型に比べて若干小さいもののほぼ正常な形態を示した。このハエを暗黒下で長期間飼育すると、緩やかにオプシンが減少するとともに、ラブドメアの微絨毛膜が細胞質へ大きく陥入して、ラブドメアの崩壊が起り、網膜変性と呼ばれる症状を示すことが明らかとなった。さらに、このハエに光を照射すると網膜変性が著しく促進され、約24時間以内にはほぼ完全に成熟ロドプシンが失われた。反応性の異なる2種類の抗ロドプシン抗体を用いた実験から、ロドプシンは光照射後急激に分解・消失するのではなく、オプシンのC末端部分がまず少し切られた状態で蓄積することがわかった。さらに、視細胞の微細形態の変化を時間を追って観察したところ、光照射後約1時間の白色光照射によりラブドメアの微絨毛膜が細胞質中に陥入しはじめ、引き続き光照射を行なうと、ラブドメアの崩壊が進行して、ラブドメア由来と考えられる異常な膜構造が細胞内に多数現れた。48時間の光照射ではラブドメアがほぼ消失すると共に、細胞体の胞状化が進行し、最終的には細胞の収縮や崩壊が観察された。また、変性中の細胞の核内には電子密度の高い異常な構造が現れ、クロマチン構造の変化が示唆された。このハエの変異形質は野生型に対して劣性であり、網膜の電気生理学的光応答も正常であったことから、光情報伝達系の亢進異常が変性の原因ではないことが示唆された。この変異は網膜変性を引き起こす変異のなかでも劣性であるという点で珍しく、またロドプシンの合成量が比較的多く変性の進行が速いという点でも他の変異とは異なる特徴を示す。このことは他の優性の網膜変性とは異なる機構で網膜変性を引き起こす可能性を示唆している。N196I変異ロドプシンは恐らくその分子構造の異常から、光受容膜の形態維持と視細胞の生存にとって悪影響を及ぼし、さらに光受容に伴う分子構造の変化によりその傾向が強められるのではないかと考えられる。

【おわりに】

本研究では、ロドプシン細胞外領域のN-結合型糖鎖結合部位がAsn20であることを決定し、それがロドプシンの成熟過程に必要な構造であることを明らかにした。また、細胞外領域において網膜変性の原因となる劣性の変異を新たに見いだした。加えて、この網膜変性が光により著しく亢進され、劇的な膜構造の変化を引き起こし、最終的には細胞死の様相を呈することを示した。

網膜変性は、ヒトの網膜色素変性症（Retinitis Pigmentosa）でも観察され、その原因の多くがロドプシンや光情報変換に関わる他のタンパク質遺伝子の変異にあることが知られている。本研究で見いだされた *ninaE^{N196I}* 等のショウジョウバエ変異体を用いた研究により、網膜変性とその光依存性のメカニズムについて解明することが可能であると考えられる。

Acknowledgments

I would like to express my great appreciation to Prof. Fumio Tokunaga and Dr. Koichi Ozaki for their constant guidance and encouragement throughout this study. I am especially grateful to Dr. Kunio Isono of Tohoku Univ. for gifts of fly stocks and useful advice for mating scheme of flies and Dr. J. E. O'Tousa of Notre Dame Univ. for *Drosophila* transformation and gifts of fly stocks and the antiserum, and Dr. Kentaro Arikawa of Yokohama City Univ. for his technical guidance on electron microscopy. I wish to thank Dr. Yuji Kito and Dr. Mikio Kataoka for their useful advise and encouragement, Dr. Osamu Hisatomi and Dr. Mamiko Ozaki for their helpful advise for various experimental techniques, Prof. Satoru Kawamura and all members of Tokunaga's Lab. and Kawamura's Lab. for their useful discussion and suggestion.

I also thank all my friends for their encouragement. Last of all, I appreciate my parents for their moral and financial support for a long time.

January 1998

Kimiaki Katanosaka